Peripheral innate immune and bacterial signals relate to clinical heterogeneity in Parkinson's disease

Ruwani S. Wijeyekoon[a*], Deborah Kronenberg-Versteeg[b], Kirsten M. Scott[a], Shaista Hayat[a], Wei-Li Kuan[a], Jonathan R. Evans[a,c], David P. Breen[d,e,f], Gemma Cummins[a], Joanne L. Jones[g], Menna R. Clatworthy[h], R. Andres Floto[h], Roger A. Barker[a,b], Caroline H. Williams-Gray[a]

a John van Geest Centre for Brain Repair, Department of Clinical Neurosciences, University of Cambridge, E.D. Adrian Building, Forvie Site, Robinson Way, Cambridge CB2 0PY, UK

b Wellcome Trust-MRC Cambridge Stem Cell Institute, University of Cambridge, Cambridge, UK

c Nottingham University Hospital NHS Trust, Nottingham, UK

d Centre for Clinical Brain Sciences, University of Edinburgh, Chancellor's Building, 49, Little France Crescent, Edinburgh, EH16 4SB, UK

e Anne Rowling Regenerative Neurology Clinic, University of Edinburgh, Chancellor's Building, 49, Little France Crescent, Edinburgh, EH16 4SB, UK

f Usher Institute of Population Health Sciences and Informatics, University of Edinburgh, 9, Little France Road, Edinburgh BioQuarter, Edinburgh, EH16 4UX, UK.

g Department of Clinical Neurosciences, University of Cambridge, Cambridge, UK

h Department of Medicine, University of Cambridge, Cambridge, UK

*Corresponding Author; Email - rsw27@cam.ac.uk

Word Count - 5843

Highlights

*Disease relevant innate immune monocyte markers are altered in Parkinson's disease

*The monocyte marker changes are accompanied by elevated serum bacterial endotoxin

*These findings are most pronounced in Parkinson's cases at higher dementia risk

*Alpha-synuclein and caspase-1 are correlated and are lower in Parkinson's serum

Abstract

The innate immune system is implicated in Parkinson's disease (PD), but peripheral *in-vivo* clinical evidence of the components and driving mechanisms involved and their relationship with clinical heterogeneity and progression to dementia remain poorly explored.

We examined changes in peripheral innate immune-related markers in PD cases (n=41) stratified according to risk of developing early dementia. 'Higher Risk'(HR) (n=23) and 'Lower Risk' (LR) (n=18) groups were defined according to neuropsychological predictors and *MAPT* H1/H2 genotype, and compared to age, gender and genotype-matched controls. Monocyte subsets and expression of key surface markers were measured using flow cytometry. Serum markers including alpha-synuclein, inflammasome-related caspase-1 and bacterial translocation-related endotoxin were measured using quantitative immuno-based assays. Specific markers were further investigated using monocyte assays and validated in plasma samples from a larger incident PD cohort (n=95).

We found that classical monocyte frequency was elevated in PD cases compared to controls, driven predominantly by the HR group, in whom Toll-Like Receptor (TLR)4+ monocytes and monocyte Triggering Receptor Expressed on Myeloid cells-2 (TREM2) expression were also increased. Monocyte Human Leukocyte Antigen (HLA)-DR expression correlated with clinical variables, with lower levels associated with worse cognitive/motor performance. Notably, monocyte changes were accompanied by elevated serum bacterial endotoxin, again predominantly in the HR group.

Serum alpha-synuclein and inflammasome-related caspase-1 were decreased in PD cases compared to controls regardless of group, with decreased monocyte alpha-synuclein secretion

in HR cases. Further, alpha-synuclein and caspase-1 correlated positively in serum and monocyte lysates, and in plasma from the larger cohort, though no associations were seen with baseline or 36-month longitudinal clinical data.

Principal Components Analysis of all monocyte and significant serum markers indicated 3 major components. Component 1 (alpha-synuclein, caspase-1, TLR2+ monocytes) differentiated PD cases and controls in both groups, while Component 2 (endotoxin, monocyte TREM2, alpha-synuclein) did so predominantly in the HR group. Component 3 (classical monocytes, alpha-synuclein) also differentiated cases and controls overall in both groups.

These findings demonstrate that systemic innate immune changes are present in PD and are greatest in those at higher risk of rapid progression to dementia. Markers associated with PD per-se (alpha-synuclein, caspase-1), differ from those related to cognitive progression and clinical heterogeneity (endotoxin, TREM2, TLR4, classical monocytes, HLA-DR), with mechanistic and therapeutic implications. Alpha-synuclein and caspase-1 are associated, suggesting inflammasome involvement common to all PD, while bacterial translocation associated changes may contribute towards progression to Parkinson's dementia. Additionally, HLA-DR-associated variations in antigen presentation/clearance may modulate existing clinical disease.

Key words

Parkinson's disease, heterogeneity, innate immune system, monocyte, alpha-synuclein, endotoxin, caspase-1

Abbreviations

ACE-R – Addenbrooke's Cognitive Examination – Revised

CIRS - Cumulative Illness Rating Scale

CNS – Central Nervous System

CSF – Cerebrospinal fluid

HR – Higher Dementia Risk

HY – Hoehn and Yahr

LR – Lower Dementia Risk

MDS-UPDRS - Movement Disorder Society – Unified Parkinson's Disease Rating Scale.

PBMC – Peripheral blood mononuclear cells

PCA - Principal Components Analysis

PD – Parkinson's Disease

1. Introduction

Parkinson's disease (PD) is clinically and pathologically heterogeneous (Rajput et al., 2009)(Kehagia et al., 2010)(Greenland et al., 2019). Clinical and genetic factors at diagnosis are known to predict the rate of progression to dementia, which affects around 50% of patients by 10 years (Williams-Gray et al., 2013). However, the biological drivers of heterogeneity in progression rates are not fully understood, and are likely to be complex, arising from interactions between genetic and environmental risk factors acting at multiple levels.

Mounting evidence from several fields has implicated involvement of the immune system in PD, however the precise components and mechanisms involved and their relationships with clinical heterogeneity and progression to dementia remain poorly understood. Genetic studies have indicated associations between immune related gene variants and PD risk (e.g. Human Leukocyte Antigen-DR (HLA-DR), Triggering Receptor Expressed on Myeloid cells-2 (TREM2), Toll-like receptor 4 (TLR4) (Nalls *et a l.*, 2011)(Hamza et al., 2010)(Rayaprolu et al., 2013)(Zhao et al., 2015)), while established PD related genes such as Leucine Rich Repeat Kinase 2 (LRRK2) have demonstrated involvement in the innate immune system (H. Lee et al., 2017) and immune-mediated conditions such as inflammatory bowel disease (Dzamko, 2017). Epidemiological studies have suggested a decreased risk of PD with anti-inflammatory and immunosuppressant drug use (X. Gao et al., 2011)(Ju et al., 2019)(Racette et al., 2018) and increased risk with immune-related conditions such as autoimmune diseases (Chang et al., 2018) and infections (Pakpoor et al., 2017)(Vlajinac et al., 2013). Animal models have also suggested involvement of the immune system in driving PD pathology, with systemic lipopolysaccharide (LPS) administration (H.-M. Gao et al., 2011) worsening alpha-synuclein pathology. Mice lacking mature T and B lymphocytes (Brochard et al., 2009) have decreased cell loss in a toxin-based model of PD and Central Nervous System (CNS) infiltration of C-C

motif chemokine Receptor2+ (CCR2+) monocytes (Harms et al., 2017) has also been shown to influence disease pathology and expression.

In the human PD brain, microglial activation has been demonstrated, both at post mortem (McGeer and McGeer, 2008) and *in-vivo* using Positron Emission Tomography (PET) neuroimaging (Gerhard et al., 2006). Several studies have also identified peripheral immune changes in PD patients, including increases in serum and secreted cytokines (e.g. Tumour Necrosis Factor (TNF)-α, Interleukin (IL)-1β, IL-2 and IL-10) (Williams-Gray et al., 2016)(Qin et al., 2016)(Sulzer et al., 2017), and associations between a more 'pro-inflammatory' cytokine profile at diagnosis and faster motor progression and impaired cognition over 3 years follow-up (Williams-Gray et al., 2016).

Many immune components are likely to play a role, and studies have demonstrated changes in adaptive immune factors such as variations in T lymphocyte subtypes and function (Baba et al., 2005)(Cen et al., 2017)(Sulzer et al., 2017)(Williams-Gray et al., 2018), decreased B lymphocytes (Stevens et al., 2012) and alterations in serum antibody levels (Scott et al., 2018) in PD. However, many of the key genetic links (HLA-DR, TREM2, TLR4) and imaging evidence have implicated specific involvement of the 'innate' immune system. In addition to central microglial activation, innate immune abnormalities have been seen in the cerebrospinal fluid (Schröder et al., 2018) and the periphery, with changes in monocyte subtype and marker expression (Grozdanov et al., 2014)(Funk et al., 2013). Studies have specifically found increased numbers of classical monocytes, increased monocyte CCR2, TLR2 and TLR4 expression (Funk et al., 2013)(Drouin-Ouellet et al., 2015), enhanced phagocytosis (Grozdanov et al., 2014)(Gardai et al., 2013)(Wijeyekoon et al., 2018) and reduced viability in culture (Nissen et al., 2019).

There is also increasing evidence that alpha-synuclein, the key pathological protein in PD, can be influenced by, and exert influence on, innate immune pathways and related microbial factors. Microbial involvement has been shown to influence disease pathology (Sampson et al., 2016) and alpha-synuclein itself may be produced, altered or trafficked in response to microbial/immune related challenges including bacterial endotoxin (Forsyth et al., 2011)(Stolzenberg et al., 2017)(Wang et al., 2016). Caspase-1, a key component of the innate immune inflammasome pathway (which is activated by a range of damage and pathogen associated molecular patterns (DAMPs/PAMPs)), can cleave alpha-synuclein and make it more aggregable, while Lewy bodies have been found to stain for caspase-1 together with alpha-synuclein (Wang et al., 2016). Forms of alpha-synuclein are also capable of activating the TLR and inflammasome pathways, leading to further cytokine production and inflammation (Codolo et al., 2013)(Gustot et al., 2015)(Kim et al., 2013)(White et al., 2018)(Grozdanov et al., 2019).

Although these lines of evidence implicate the innate immune system in PD, there has been limited characterisation of systemic innate immune and associated factors and their relevance to clinical heterogeneity and disease progression rate, in clinical PD cases. Consequently, we sought to pursue such an investigation, by characterising relevant peripheral innate immune components in the blood of a cohort of early-moderate stage PD cases stratified around risk for early dementia and paired matched controls without neurological disease. We also investigated blood samples for the presence of factors implicated in driving the innate immune changes in PD, including alpha-synuclein and bacterial endotoxin. We used a data driven approach to explore the relationships between these factors and innate immune changes and assessed links with disease status and dementia risk.

2. Materials and Methods

2.1 Participants

Ethical approval was obtained from the Cambridgeshire Research Ethics Committee and written consent was obtained from participants in compliance with the Declaration of Helsinki. Parkinson's cases were recruited from the PD Research Clinic at the John van Geest Centre for Brain Repair, University of Cambridge.

Inclusion criteria comprised satisfying UK Brain Bank Criteria for Parkinson's disease, age 55-80 and Hoehn and Yahr (HY) stage ≤ 2.

In order to classify patients *a priori* according to their risk of progression to dementia, the study utilised factors previously identified from the CamPaIGN longitudinal cohort study (semantic fluency score <20, impaired pentagon copying and H1/H1 *MAPT* haplotype)(Williams-Gray et al., 2009)(Williams-Gray et al., 2013). Each factor contributes significantly to increased dementia risk at 10 years, with a hazard ratio of 3.05 for semantic fluency <20, 2.55 for impaired pentagon copying and 3.08 for Microtubule Associated Protein Tau *(MAPT)* H1/H1(Williams-Gray et al., 2013).

The 'Higher Dementia Risk' (HR) group had at least one of these factors at diagnosis, while the 'Lower Dementia Risk' (LR) group had none.

Age, gender and *MAPT*-genotype matched controls, with no history of neurological disease, self-reported memory problems or depression were recruited via the Cambridge Bioresource(http://www.cambridgebioresource.org.uk).

Exclusion criteria for all participants consisted of the presence of-: another neurodegenerative, chronic inflammatory or autoimmune disorder, current clinically significant infection, surgery within last month, vaccinations in the last 3 weeks, use of steroids (within last 3 months), aspirin >75mg or ibuprofen/nonsteroidal anti-inflammatory drugs (within 2 weeks) or long-term immunosuppressant drugs (within 1 year).

2.2 Clinical data acquisition and sample collection

Participants attended for three visits at monthly intervals. Data gathered included demographic data, medical and drug history and comorbidity status (Cumulative Illness Rating Scale (CIRS)(Parmelee et al., 1995)). Verbal screening for inter-current infections was performed to avoid sampling during periods of illness. Clinical assessments included the Movement Disorder Society-Unified Parkinson's Disease Rating Scale (MDS-UPDRS), HY scale, Addenbrooke's Cognitive Examination-Revised (ACE-R), semantic fluency (animals in 90s) and pentagon copying.

Venous blood (up to 50ml) was sampled at each visit and used for serum extraction and/or Peripheral Blood Mononuclear Cell (PBMC) isolation and subsequent ex-vivo immunocytochemistry/flow cytometry or CD14+ cell separation. All samples were collected between 9.00 and 11.00am, with no imposed medication changes. PD/control samples paired by age, gender and genotype were processed in parallel on the same day.

2.3 Sample Processing

2.3.1 PBMC isolation, Immunocytochemistry and Flow Cytometry

PBMCs were extracted using the standard Ficoll gradient method and subjected to immunocytochemistry and flow cytometry as previously described (Appendix A) (Wijeyekoon et al., 2018), to measure key monocyte cell surface markers.

The antibody panel used for flow cytometry consisted of CD14 – APC-H7, CD16 – PerCP-Cy5.5, HLA-DR – BV605, TREM2 –APC, TLR2 – PE, TLR4 – BV421 (Table A.1). Monocytes were gated and analysed as described in the literature (Ziegler-Heitbrock and Hofer, 2013)(Fig. 1A) and as detailed in Appendix A.

2.3.2 Serum sample processing and assays

Blood samples for serum collection were left to clot for 15 minutes and centrifuged at 2000rpm for 15 minutes at room temperature. The separated serum was stored in 200-400 µl aliquots, frozen at -80°C and thawed before use. The following assays were performed (see Appendix A for further details).

Mesoscale Discovery (MSD) platform electrochemiluminescence assays

Samples from each of the 3 visits were processed in duplicate according to the manufacturer's instructions for the MSD V-Plex 10-spot Pro-inflammatory panel 1 assay (Interferon(IFN)-γ, IL-1β, IL-2, IL-4, IL-6, IL-8, IL-10, IL-12p70, IL-13 and TNFα; 1:2 dilution; 50ul per well); MSD V-Plex Human C-Reactive Protein (CRP) assay (1:1000 dilution; 25ul per well); MSD Human Alpha-Synuclein Assay (1:10 dilution; 25ul per well).

Readings were obtained using the MSD SECTOR Imager. Data was exported and analysed using the MSD Discovery Workbench software.

Additional assays -: Caspase-1, soluble CD14, soluble TREM2 and bacterial endotoxin

Additional markers were measured from remaining serum aliquots and included-: caspase-1 (Wang et al., 2016)(Codolo et al., 2013); bacterial endotoxin (a primary ligand for TLR4) and soluble CD14, as markers of microbial translocation (Morris et al., 2015)(Kelesidis et al., 2012); and soluble TREM2, as an indicator of TREM2 shedding (Feuerbach et al., 2017).

Samples were analysed in duplicate using ELISA assays for caspase-1(R and D Systems) (2:3 dilution), soluble TREM2(Cloud-Clone Corp.)(1:2 dilution), and soluble CD14(R and D systems) (1:800 dilution), following the manufacturer's instructions (Appendix A).

Serum endotoxin was measured using the Pierce Limulus Amoebocyte Lysate (LAL) Chromogenic Endotoxin Quantitation Kit (Thermo Scientific) (40 samples) and the LAL Chromogenic Endpoint Assay (Hycult Biotech) (36 samples), due to supplier shortages of the former during the course of the study. Samples from PD and control pairs were analysed using the same plate and kit. The results from both batches covered similar ranges (Thermo Scientific kit – 0.46 – 6.32 EU/ml; Hycult Biotech kit – 0.46 – 5.00 EU/ml). All samples were assayed in duplicate according to the manufacturer's instructions, with 1:50 dilution.

2.3.3 Monocyte separation

Monocytes were separated using MACS® CD14 magnetic beads (Miltenyi Biotec) as per the manufacturer's instructions and as previously detailed (Appendix A)(Wijeyekoon et al., 2018).

2.3.4 Fluorescent alpha-synuclein endocytosis assays

Monocyte uptake of recombinant human alpha-synuclein (1-140) HiLyte^{TM} Fluor 488 (Anaspec) was assessed in standard medium (clear Roswell Park Memorial Institute (RPMI) culture medium and 10% Foetal Calf Serum (FCS)), and in autologous serum (Appendix A). Titration and time course experiments were performed prior to study commencement, to optimise concentrations and end time points. Final assays were run using 10,000ng/ml of alpha-synuclein for an incubation period of 90 minutes. Alpha-synuclein uptake was assessed and quantified using flow cytometry. Representative post-uptake monocyte samples were used for imaging using fluorescence microscopy.

2.3.5 Monocyte alpha-synuclein and caspase-1 secretion assays

Separated monocytes were cultured in RPMI and 10% FCS under standard conditions at a concentration of $1x10^6$ cells per ml per well, with and without LPS (1ng/ml). Paired PD and control cultures, with and without LPS, were performed in parallel. The supernatant was collected at 24h, aliquoted and stored at -80ºC.

Supernatants were analysed for alpha-synuclein and caspase-1 according to the manufacturer's instructions as detailed above and in Appendix A. Supernatants were diluted 1:10 for alpha-synuclein and 2:3 for caspase-1 in the appropriate buffers and were assayed in duplicate.

2.3.6 Monocyte Lysates

Monocytes were lysed in homogenisation solution (Appendix A), and their total protein concentration was measured using a Bicinchoninic acid (BCA) assay (Appendix A). Alpha-synuclein and caspase-1 levels were measured in monocyte lysates using the assays and dilutions described above. Western blots for alpha-synuclein and caspase-1 were performed on the monocyte lysates, with β-actin as loading control (Appendix A).

2.4 Statistical analysis

Data was analysed using IBM SPSS version 25 or GraphPad Prism 7. Experimental outliers >3 standard deviations (SD) above or below the mean were excluded and normality was assessed using the Shapiro-Wilk test prior to analysis. Due to the paired experimental methodology, group comparisons were performed for PD cases overall and within each *a priori* determined risk group versus paired controls using paired two-tailed t-tests (parametric) or Wilcoxon matched-pairs tests (non-parametric) as appropriate. Bonferroni correction for multiple testing was used across each assay category (e.g. monocyte subtypes, monocyte surface expression markers, all serum assays). All monocyte markers and serum markers with a PD-Control uncorrected significant difference of $p<0.05$ were included in a Principal Components Analysis (PCA).

Relationships between monocyte/serum markers and clinical variables (MDS-UPDRS motor, ACE-R and semantic fluency scores) were assessed using bivariate correlation analysis. Markers reaching significance ($p<0.05$) were included in multiple regression analyses for each clinical variable with appropriate confounders. Correlations between PCA component scores and clinical variables were compared using similar methods.

2.5 Plasma markers and disease progression

Stored baseline plasma samples were available for another cohort of 93 patients (Incidence of Cognitive Impairment in Cohorts with Longitudinal Evaluation in Parkinson's Disease (ICICLE-PD) Cambridge cohort) who were newly diagnosed with PD and recruited between 2009 and 2011 from community/outpatient clinics in Cambridge, United Kingdom. Details of recruitment, assessment and follow up of the patients have been previously published (Yarnall

et al., 2014). Subjects were assessed clinically as previously described (Williams-Gray et al., 2016), at baseline, 18 and 36 months.

Venous blood samples (EDTA tubes) were obtained at baseline entry to the study and plasma extracted by centrifugation (2000rpm for 15 minutes), with storage at -80ºC. On use, plasma was thawed and processed for alpha-synuclein and caspase-1(1:50 dilution)(Appendix A).

Relationships between baseline plasma markers and longitudinal clinical progression were analysed using simple bivariate correlation analyses. Significant correlations were further examined using multiple regression analyses with relevant confounders.

2.6 Data availability

Data related to the findings of this study will be available from the corresponding author, upon reasonable request.

3. Results

3.1 Participants

41 Parkinson's disease cases and 41 paired matched controls were recruited (23 pairs HR group and 18 pairs LR group) (Table 1).

Variable	Higher Risk (HR) Group			Lower Risk (LR) Group			HR vs LR Parkinson's disease p
	Parkinson's disease	Paired Controls	p	Parkinson's disease	Paired Controls	p	
Number (n)	23	23		18	18		
Age (years)	70.13± 5.96	69.43± 5.40	0.680	66.33 ± 6.36	66.39± 5.71	0.978	0.056
Gender (% male)	73.9	73.9	0.631	61.1	61.1	0.633	0.295
Disease Duration (years)	4.26 ± 1.09			4.26 ± 1.23			0.994
MDS-UPDRS motor score	38.35± 12.71			31.00 ± 10.78			0.062
Equivalent Levodopa dose	493.34 ± 269.78			717.03 ± 279.27			0.013*
ACE-R score	89.96± 9.94			96.88±2.31			0.008*
CIRS Total Score	4.30 ± 2.05			5.39 ± 2.99			0.177

Table 1 – Demographic details of participant groups *(Mean ± Standard Deviation). *p<0.05. MDS-UPDRS – Movement Disorder Society Unified Parkinson's Disease Rating Scale; ACE-R – Addenbrooke's Cognitive Examination- Revised; CIRS – Cumulative Illness Rating Scale.*

3.2 Monocyte markers

There were no significant differences in total monocytes (as a percentage of PBMCs) between PD and paired controls, overall ($t(40)=0.5446$, $p=0.5891$) nor in both risk groups (Fig.1B). PD cases had a statistically significant (withstanding Bonferroni correction for multiple testing) higher proportion of classical monocytes ($W=-445$, $p=0.0014$), with trends (uncorrected significance) towards correspondingly lower intermediate ($t(37)=2.334$, $p=0.0251$) and non-classical ($W=278$, $p=0.0433$) monocytes, compared to paired controls (Fig.1C-E). Risk group analysis revealed a trend towards higher classical monocyte percentages in the HR PD group ($W= -141$, $p=0.0127$) compared to paired controls, but not the LR group (Fig.1C).

TLR4+ monocytes constituted a higher percentage in PD compared to controls ($W= -204$, $p=0.0128$), with statistical significance in the HR PD group ($W= -124$, $p=0.0004$). The percentage of TLR2+ monocytes was also significantly higher in all PD cases ($W= -347$, $p=0.0078$)compared to controls and within the HR PD group ($W= -134$, $p=0.0107$) (Fig.2A-D).

Monocyte TREM2 and HLA-DR measures did not differ between PD cases and controls. However, HR group PD cases had significantly higher monocyte TREM2 expression ($t(19)=2.977$, $p=0.0077$) compared to paired controls and a trend towards a higher percentage of TREM2+ monocytes ($t(20)=2.216$, $p=0.0385$), while LR PD cases demonstrated a trend towards a lower percentage of TREM2+ monocytes ($t(17)=2.457$, $p=0.0250$) (Fig.2E-H).

Additional analyses performed on the Classical monocyte sub-population indicated similar patterns of changes to Total monocytes in all measured markers, but with decreased

significance overall, possibly due to smaller cell numbers within the subpopulation (Appendix A, Figure A.5).

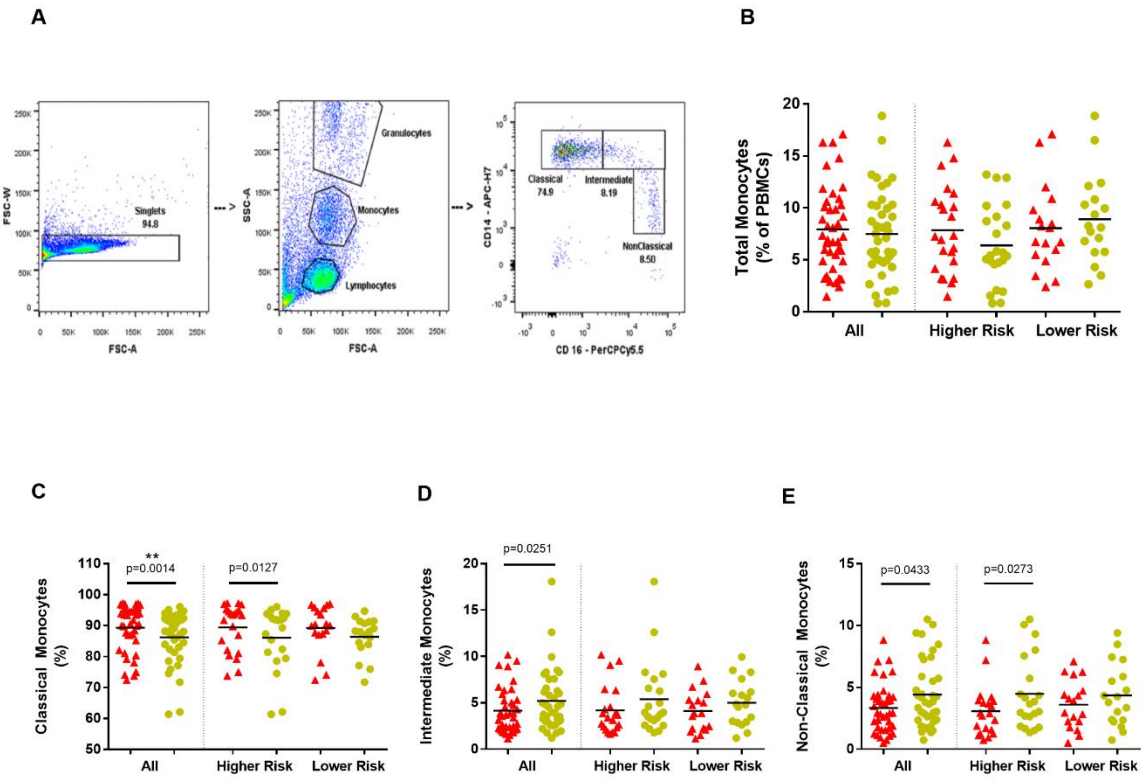

Figure 1 – Monocyte subtypes

(A) - Flow cytometry gating strategy for monocytes and monocyte subtypes *Singlets are identified by plotting Forward Scatter-Area (FSC-A) versus Forward Scatter-Width (FSC-W) and excluding cells with multiples of a single width size. Monocyte are broadly distinguished using tight gates based on FSC-A (size) and Side Scatter-Area (SSC-A) (granularity/internal complexity). Monocyte subtypes are distinguished based on CD14 and CD16 expression – Classical (CD14 high, CD16 negative); Intermediate (CD14 high, CD16 positive); Non-Classical (CD14 low, CD16 high).*

(B) - Total monocytes (as a percentage of PBMCs) in all patients and controls; overall and within dementia risk groups. (Parkinson's disease=red; Controls=yellow).

*(C),(D),(E)-Monocyte Subtypes. (C) Classical, (D) Intermediate and (E) Non-Classical monocytes (as percentage of total monocytes) in Parkinson's disease patients and controls; overall and within dementia risk groups. (Parkinson's disease=red; Controls=yellow). **significance withstood Bonferroni correction for multiple testing within the relevant category.*

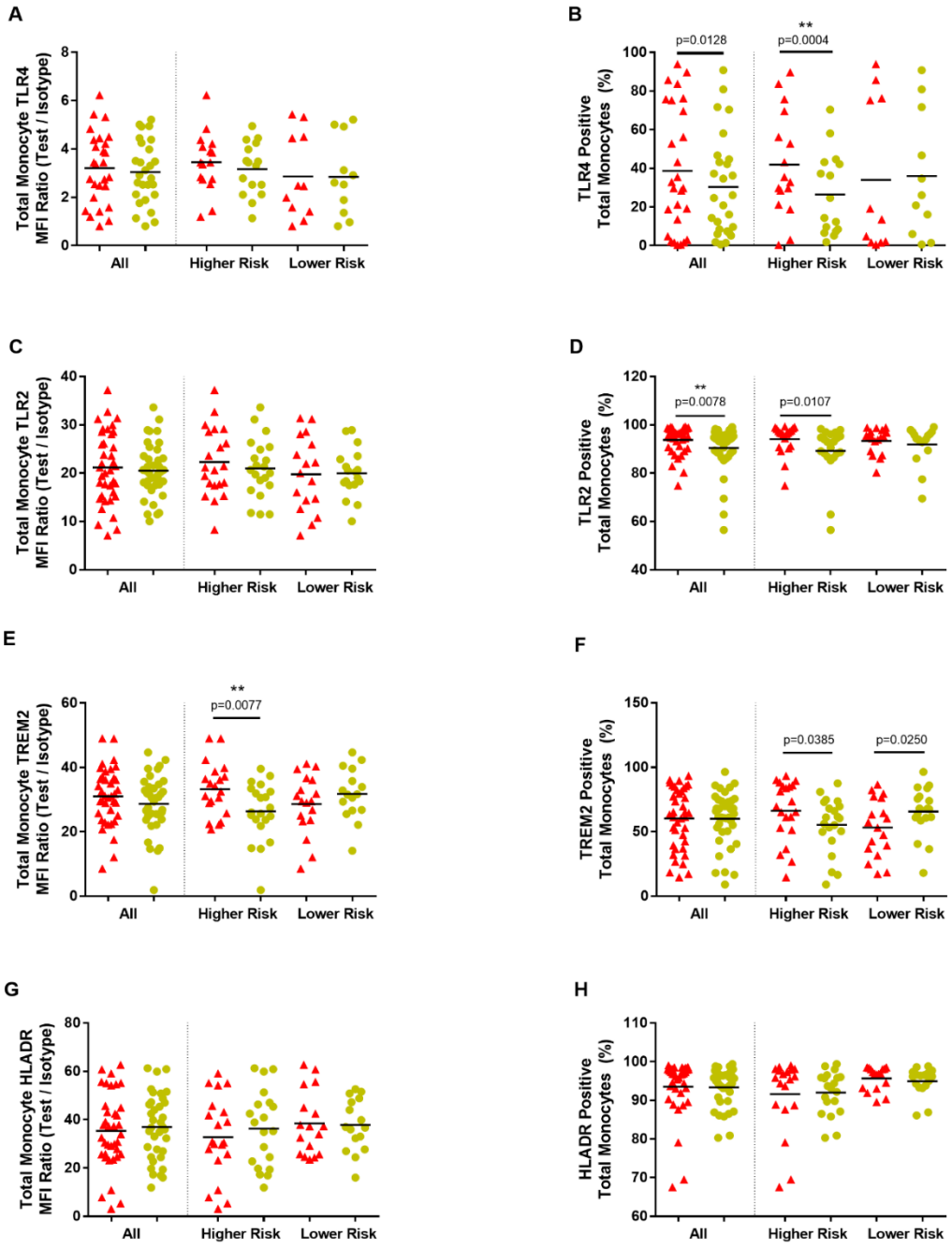

Figure 2 – Monocyte surface markers

*Total monocyte marker expression in Parkinson's disease cases versus paired controls; overall and within risk groups. Graphs showing total monocyte MFI (Median Fluorescence Intensity) ratios (Test/Isotype) ((A), (C), (E), (G)) and percentage monocytes positive ((B), (D), (F), (H)). (Parkinson's disease=red; Controls=yellow). **significance withstood Bonferroni correction for multiple testing within the relevant category.*

3.3 Monocyte markers and clinical variables

Monocyte HLA-DR surface expression levels correlated with better cognitive function (higher ACE-R ($r=0.402$, $p=0.015$) and semantic fluency ($r=0.440$, $p=0.006$)) and motor function (lower UPDRS motor score ($r=-0.398$, $p=0.016$)). There were no correlations with levodopa equivalent dose, suggesting the associations were unlikely to be medication driven (Fig.3). There were no significant correlations between clinical scores and other monocyte marker measures (data not shown).

Multivariate regression analysis with the UPDRS motor score, semantic fluency or ACE-R scores as the dependent variables, and age, disease duration, levodopa equivalent dose and CIRS comorbidity score as potential confounders, confirmed the relationships with total monocyte HLA-DR surface expression level (Table A.2).

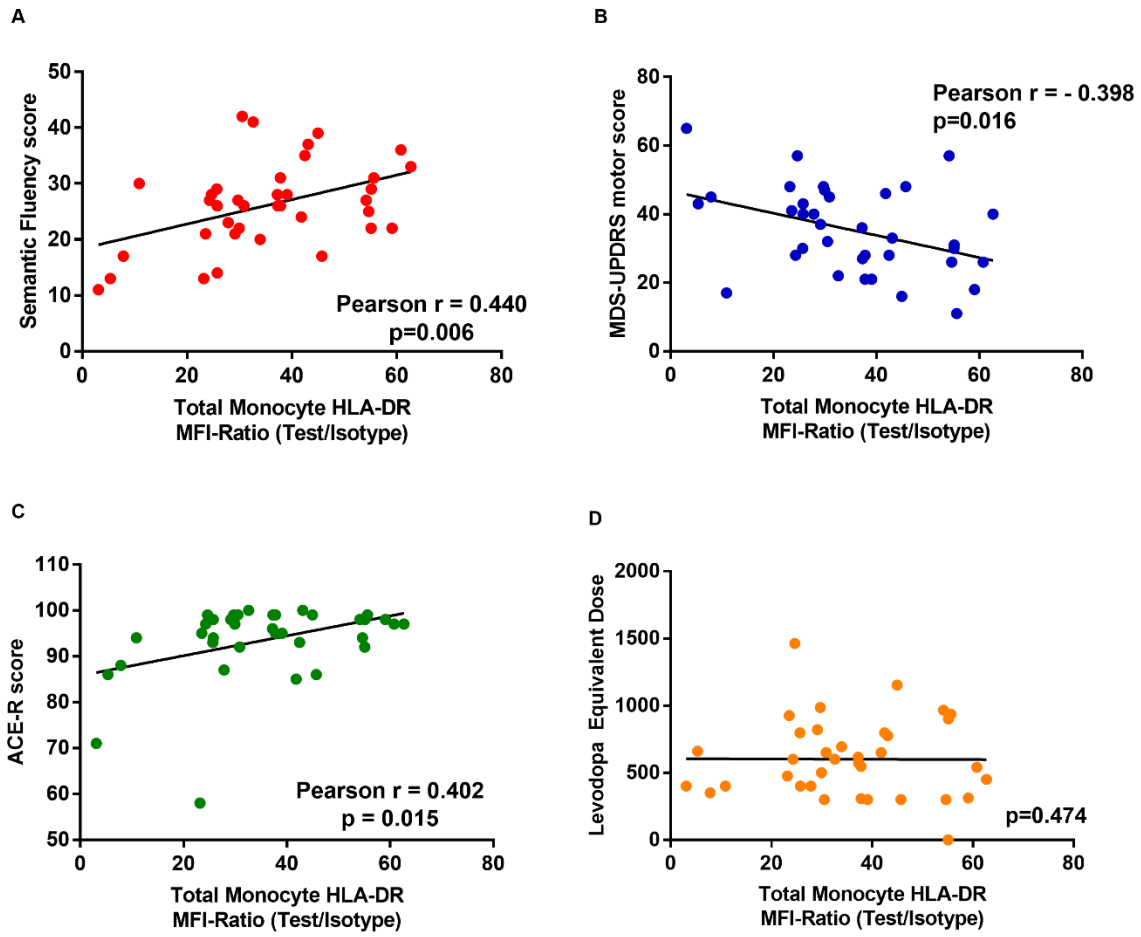

Figure 3 – Monocyte HLA-DR expression and clinical data

Relationships between Total Monocyte HLA-DR expression (Test/Isotype MFI Ratio) and clinical data - (A) Semantic Fluency. (B) MDS-UPDRS III motor score. (C) ACE-R score. (D) Absence of correlation with Levodopa equivalent dose.

3.4 Serum markers

Serum alpha-synuclein concentration was significantly lower in PD cases compared to controls, regardless of risk group (Overall W=810, p<0.0001; HR W=276, p<0.0001; LR W=147, p<0.0001)(Fig.4A).

Serum caspase-1 was also significantly lower in PD compared to controls, regardless of risk group (Overall W=596, p<0.0001; HR W=139, p=0.0013; LR W=161, p<0.0001) (Fig.4B).

Serum endotoxin was higher in PD compared to controls (W=-287, p=0.0231), with a non-significant trend in the HR group (W=-79, p=0.0898) (Fig.4C).

Serum IL-2 and IFN-γ displayed trends towards decrease in the HR-PD group, but there were no statistically significant case-control differences in the serum concentrations of measured cytokines, CRP, soluble CD14 or soluble TREM2 in patients compared to controls (Tables A.3 and A.4; Fig.4D,E).

For both monocyte markers and serum variables, gender-stratified paired comparisons indicated overall similar trends in all markers within both genders, though significance was greater in the male group, which may relate to the larger sample size (>68% male)(data not shown).

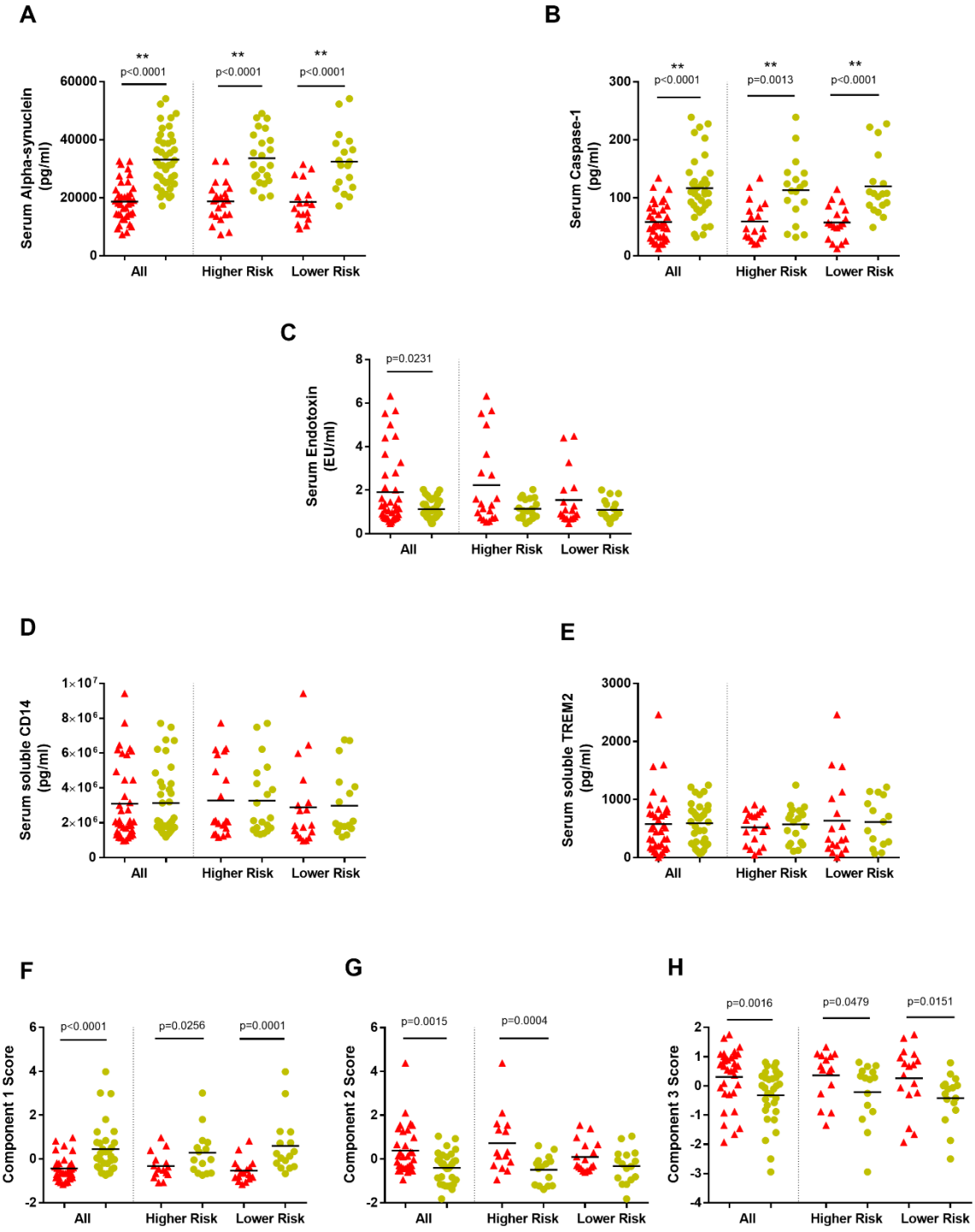
A
Serum Alpha-synuclein (pg/ml)
60000
40000
20000
0
**
p<0.0001
**
p<0.0001
**
p<0.0001
All
Higher Risk
Lower Risk
B
Serum Caspase-1 (pg/ml)
300
200
100
0
**
p<0.0001
**
p=0.0013
**
p<0.0001
All
Higher Risk
Lower Risk
C
Serum Endotoxin (EU/ml)
8
6
4
2
0
p=0.0231
All
Higher Risk
Lower Risk
D
Serum soluble CD14 (pg/ml)
1×10^7
8×10^6
6×10^6
4×10^6
2×10^6
0
All
Higher Risk
Lower Risk
E
Serum soluble TREM2 (pg/ml)
3000
2000
1000
0
All
Higher Risk
Lower Risk
F
Component 1 Score
6
4
2
0
-2
p<0.0001
p=0.0256
p=0.0001
All
Higher Risk
Lower Risk
G
Component 2 Score
6
4
2
0
-2
p=0.0015
p=0.0004
All
Higher Risk
Lower Risk
H
Component 3 Score
2
1
0
-1
-2
-3
-4
p=0.0016
p=0.0479
p=0.0151
All
Higher Risk
Lower Risk

Figure 4 – Serum markers and Principal Components Analysis

*(A)-(E) - Concentrations of serum (A) alpha-synuclein, (B) caspase-1, (C) endotoxin, (D) soluble CD14 and (E) soluble TREM2 in Parkinson's disease patients and controls and within Parkinson's dementia risk groups. (Patients=red; Controls=yellow). **significance withstood Bonferroni correction for multiple testing within the relevant category.*

(F)-(H) - Summary of Principal Components Analysis (PCA) component score comparisons between all Parkinson's patients and paired controls and within risk groups. (Patients=red; Controls=yellow).

Component 1 - (+)serum alpha-synuclein, (+)caspase-1 and (-)TLR2+ monocytes; Component 2 - (+)serum endotoxin, (+)monocyte TREM2 and (-)serum alpha-synuclein; Component 3 - (+)classical monocyte percentage and (-)serum alpha-synuclein.

3.5 Serum markers and clinical variables

MDS-UPDRS motor scores correlated negatively with serum alpha-synuclein (r=-0.407; p=0.010) (Fig.A.8, but this did not remain significant in a multiple regression analysis with age, disease duration, Levodopa equivalent dose and CIRS total score as potential confounders (Table A.5).

3.6 Principal Component Analysis (PCA)

In order to explore relationships between key markers, a PCA was performed, using all participant data on all monocyte markers, and serum markers with uncorrected significant results on overall PD-Control paired analysis (Appendix A).

A three-component solution cumulatively explained 67.64% of the total variance. The principal component loadings of the rotated solution are shown in Table 2. Component 1 (32.48%) was mainly driven by (+)serum alpha-synuclein, (+)caspase-1 and (-)TLR2+ monocytes.

Component 2 (19.48%) was mainly driven by (+)serum endotoxin, (+)monocyte TREM2 and less by (-)serum alpha-synuclein. Component 3 (15.67%) was mainly driven by (+)classical monocyte percentage and (-)serum alpha-synuclein.

Variable	Component 1	Component 2	Component 3	Communalities
Total Monocyte TLR2+ percentage	**-0.880**	(-0.093)	(-0.042)	0.785
Serum Caspase-1	**0.801**	(-0.275)	(-0.093)	0.726
Serum Endotoxin	(-0.120)	**0.759**	(0.056)	0.594
Total Monocyte TREM2 MFI ratio	(0.058)	**0.673**	(-0.244)	0.515
Serum Alpha-synuclein	**0.401**	**-0.536**	**-0.330**	0.558
Classical Monocyte percentage	(-0.012)	(-0.072)	**0.936**	0.881

Table 2 - Principal component loadings for the rotated solution of the PCA. *Coefficients <0.3 were suppressed and are shown in brackets.*

Paired comparisons of PCA components between PD and controls and within the risk groups (Fig.(4F),(G),(H)), indicated that Component 1 was significantly lower in all PD versus controls (W=397, p<0.0001) and in both HR (W=78, p=0.0256) and LR (W=118, p=0.0001) groups, while Component 2 was significantly higher in all PD versus controls (W=-299, p=0.0015) and within the HR group (W=-112, p=0.0004). Component 3 was also significantly higher in all PD versus controls (W=-297, p=0.0016), with elevation within the LR (W=-84,

p=0.0151) and the HR (W=-70, p=0.0479) groups. Bivariate correlation analyses did not show any associations between PCA components and measured clinical variables.

Key relationships identified through PCA were further explored, including the relationship between endotoxin and TREM2 (component 2) and between alpha-synuclein and caspase-1 (component 1).

3.7 Endotoxin and TREM2

Serum endotoxin did not directly correlate with monocyte surface TREM2. However, it demonstrated a significant, but weak positive correlation with soluble TREM2 (r=0.1613, p=0.0005), which remained significant on multivariate linear regression analysis, with monocyte TREM2 and age as potential confounders (Fig.A.9; Table A.6).

3.8 Alpha-synuclein and Caspase-1

In addition to clustering within the PCA (component 1), serum alpha-synuclein and caspase-1 were significantly positively correlated with each other (r =0.382, p=0.001)(Fig.5I). In order to further investigate potential mechanistic factors relating to the serum changes seen in these proteins (e.g. differences in cellular uptake and release), additional functional assays and analyses were performed using ex-vivo monocytes from subsets of participants from the cohort.

3.8.1 Monocyte fluorescent alpha-synuclein uptake

Monocyte uptake of fluorescent monomeric alpha-synuclein was assessed using standard medium, as well as an autologous serum environment (Fig.5A-D). Autologous serum was used to better represent the *in-vivo* intravascular environment (Wijeyekoon et al., 2018), while the standard medium was used to study the intrinsic uptake ability of the monocytes independent of serum factors.

There were no significant differences in fluorescent alpha-synuclein uptake in standard medium between patients and controls (% positive monocytes $t(35)=0.7691$, $p=0.4470$)(Fig.5C,D). In autologous serum, uptake was decreased across all groups, compared to standard medium ($t(50)=46.45$, $p<0.0001$), but no significant case-control differences were seen ($t(27)=1.685$, $p=0.1034$).

3.8.2 Monocyte alpha-synuclein and caspase-1 secretion

Monocyte secretion of alpha-synuclein and caspase-1 were not significantly different between all PD and controls (Fig.5E-H). However alpha-synuclein secretion was decreased in HR cases compared to paired controls, with ($t(12)=2.324$, $p=0.0385$) and without LPS stimulation ($t(13)=2.555$, $p=0.0240$)(Fig.5E,G). The number of LR group pairs were insufficient for analysis.

Additionally, LPS led to increased secretion of caspase-1 overall, with no relative difference in PD versus controls (Figure 5F,H). However, alpha-synuclein secretion did not increase with LPS stimulation (Figure 5E,G).

3.8.3 Monocyte lysate alpha-synuclein and caspase-1

Western blot analysis indicated the presence of higher molecular weight alpha-synuclein and of caspase-1 in monocyte lysates in both PD and controls (Fig.A.10A,B). Measurement of total

alpha-synuclein and caspase-1 levels in monocyte lysates (relative to total protein) using MSD and ELISA assays, found no significant case-control differences (Fig.A.10C,D)).

However, similar to the serum findings, monocyte lysate alpha-synuclein and caspase-1 were also positively correlated with each other (r=0.603, p=0.001)(Fig.5J).

3.9 Alpha-synuclein and caspase-1 in a separate, larger incident PD cohort

Alpha-synuclein and caspase-1 were measured in baseline plasma samples from the ICICLE-Cambridge cohort (n=93; mean(standard deviation)-:age=66.73(6.92);disease duration =0.81(0.57); 60.2% male).

The two proteins again demonstrated a significant positive correlation with each other (Pearson's r=0.480, p<0.001;Fig.5K), replicating findings in the primary study cohort. There were no significant correlations between the baseline levels of either marker and baseline or longitudinal cognitive/motor measures over 36 months (data not shown).

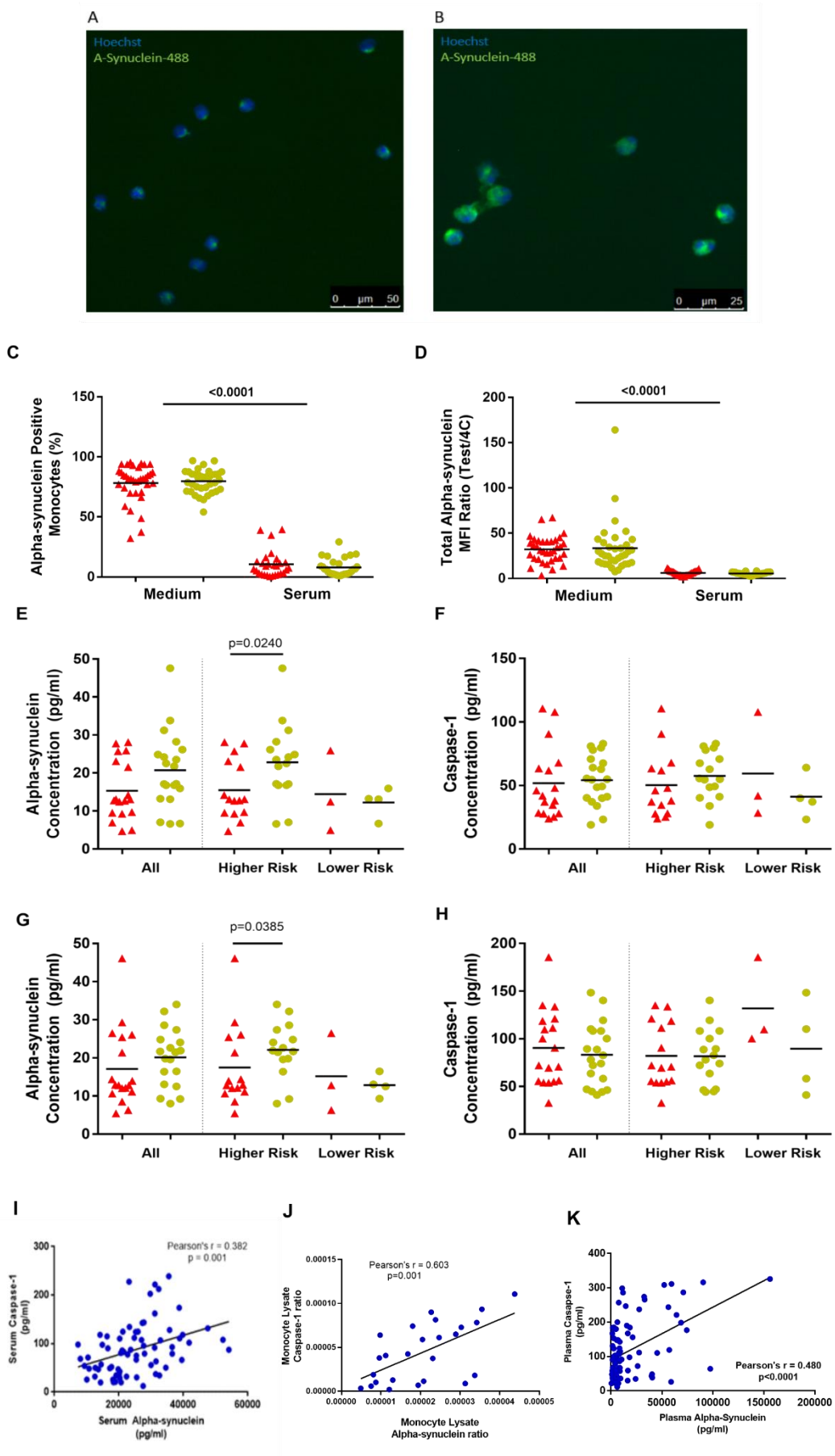
A
Hoechst
A-Synuclein-488
0 µm 50
B
Hoechst
A-Synuclein-488
0 µm 25
C
Alpha-synuclein Positive Monocytes (%)
<0.0001
Medium
Serum
D
Total Alpha-synuclein MFI Ratio (Test/4C)
<0.0001
Medium
Serum
E
Alpha-synuclein Concentration (pg/ml)
p=0.0240
All
Higher Risk
Lower Risk
F
Caspase-1 Concentration (pg/ml)
All
Higher Risk
Lower Risk
G
Alpha-synuclein Concentration (pg/ml)
p=0.0385
All
Higher Risk
Lower Risk
H
Caspase-1 Concentration (pg/ml)
All
Higher Risk
Lower Risk
I
Serum Caspase-1 (pg/ml)
Pearson's r = 0.382
p = 0.001
Serum Alpha-synuclein (pg/ml)
J
Monocyte Lysate Caspase-1 ratio
Pearson's r = 0.603
p=0.001
Monocyte Lysate Alpha-synuclein ratio
K
Plasma Casapse-1 (pg/ml)
Pearson's r = 0.480
p<0.0001
Plasma Alpha-Synuclein (pg/ml)

Figure 5 – Alpha-synuclein and Caspase-1

(A), (B) - Fluorescence microscope images of monocytes which have taken up fluorescent alpha-synuclein- HiLyte^{TM} Fluor 488 at 90minutes. Hoechst staining identifies cell nuclei. (a) 20X; (b) 40X.

(C), (D) - Monocyte fluorescent alpha-synuclein uptake in standard medium and in autologous serum – (C) percentage alpha-synuclein positive monocytes; (D) total monocyte MFI ratio. (Medium- Patients=35, Controls=35; Serum- Patients=27, Controls=28) (Patients=red; Controls=yellow).

(E),(F),(G),(H) - Alpha-synuclein and caspase-1 in monocyte 24 hour culture supernatants without (E)(F) and with (G)(H) LPS, in all participants and within risk groups. (Patients = red, Controls= yellow).
(All participants- Patients=18, Controls=20; Higher Risk Patients=15, Controls=16; Lower Risk Patients=3, Controls=4) (Patients=red; Controls=yellow).

(I), (J) Graphs showing significant relationship between alpha-synuclein and caspase-1 in serum (I) and monocyte lysates (J).

(K) ICICLE-Cambridge cohort - Relationship between alpha-synuclein and caspase-1 in plasma samples collected at study baseline.

4. Discussion

This study evaluated key peripheral innate immune markers linked to PD, in a cohort of dementia risk stratified patients and carefully matched controls. The findings confirmed that there are significant peripheral innate immune changes in PD, with increased classical monocytes and TLR positive monocytes, and further demonstrated that these changes are most marked in those individuals at increased early dementia risk. Monocyte TREM2 expression was also elevated in the higher dementia risk group, while higher monocyte HLA-DR expression correlated with better existing motor and cognitive performance.

The study has also uniquely shown that innate immune changes in PD are accompanied by elevated serum levels of bacterial endotoxin, suggesting that this may be playing a critical role in driving the innate immune response and associated pathology. In addition, serum alpha-synuclein was significantly decreased in PD, irrespective of dementia risk group and had a close relationship with serum caspase-1-a key component of the inflammasome pathway.

PCA confirmed the clustering of markers with similar patient-control group variations. In particular, component 1 was mainly driven by alpha-synuclein and caspase-1 plus monocyte TLR2 and demonstrated significant PD-control differences overall and in both risk groups. Component 2 was driven by serum endotoxin, monocyte TREM2 and serum alpha-synuclein, with significant overall PD-control differences, predominant within the HR group. Component 3 was driven by the classical monocyte percentage and serum alpha-synuclein, with significant PD-control differences also overall and within both groups.

4.1 Monocyte changes in PD

The increase in classical monocytes (with corresponding decrease in non-classical monocytes), and monocyte TLR2+ and TLR4+ monocytes observed in this PD cohort confirms previous findings (Grozdanov et al., 2014)(Drouin-Ouellet et al., 2015). However, this study further demonstrates that these changes are mainly driven by those at increased risk of dementia.

Classical monocytes (up to 85% of total monocytes) are mainly involved in phagocytosis, antigen presentation to adaptive immune cells and cytokine secretion in response to TLR stimulation (Wong et al., 2012)(Mukherjee et al., 2015), although exact subtype functions may vary under different clinical conditions (J. Lee et al., 2017)(Boyette et al., 2017). Intermediate and non-classical monocytes may also be more senescent cells, that increase with age (Ziegler-Heitbrock and Hofer, 2013) and derive from further differentiation of classical monocytes in the bone marrow (Ong et al., 2018)(Patel et al., 2017). At a systemic level, LPS stimulation leads to depletion of monocyte numbers and on recovery, classical monocytes appear to rise first (Tak et al., 2017). Thus, the increased classical monocytes seen in PD compared to controls, most prominent in the HR group, may reflect chronic exposure to the increased endotoxin, in these patients. The data is also consistent with our previous finding of reduced senescence markers in T lymphocytes in PD cases in this cohort (Williams-Gray et al., 2018).

The TLR2+ monocyte percentage varied inversely to alpha-synuclein and caspase-1 in PCA component 1. TLR2 is an innate immune receptor to DAMPs/PAMPs(e.g. bacterial-derived lipids, amyloids) and endogenous ligands including forms of alpha-synuclein (Bryant et al., 2015) (Kim et al., 2013)(Kim et al., 2016a)(Codolo et al., 2013), and can also facilitate activation of the inflammasome pathway (Rapsinski et al., 2015) and caspase-1.

TLR4 has a major role in the transduction of the cellular response to bacterial endotoxin and its stimulation leads to activation of Nuclear factor-kappa B (NF-κB) and transcription of cytokine precursors (e.g.IL-6, IL-1β) and inflammasome components (Lu et al., 2008), potentially leading to a relative 'priming' effect on inflammasome activation in patients.
Thus, the TLR2 and TLR4 monocyte changes seen may reflect increased potential to respond to DAMPS/PAMPS including alpha-synuclein, with subsequent promotion of caspase-1 activation, intracellular accumulation/aggregation and inflammation, mainly in the HR patients.

Significant elevation of monocyte TREM2 was also observed in the HR patient group. TREM2 is involved in bacterial clearance during sepsis (Chen et al., 2013) and may have a role in regulating TLR pathway signalling (Hamerman et al., 2006)(Kober and Brett, 2017). Increased monocyte TREM2 expression is seen in Alzheimer's disease (Hu et al., 2014) and TREM2 can act as a microglial receptor for amyloid-beta, with involvement in phagocytosis and clearance of Alzheimer's pathology (Zhao et al., 2018)(Lee et al., 2018). Interestingly, this may suggest that TREM2 may be raised in response to chronic TLR stimulation and indicates possible immunological similarities between high dementia risk PD and Alzheimer's disease.

Monocyte HLA-DR expression did not differ between PD cases and controls, but did significantly correlate with clinical variables in disease (lower levels associated with worse cognitive/motor function). Low monocyte HLA-DR is a key feature of monocyte tolerance, typically known to occur subsequent to stimuli such as LPS/endotoxin or sepsis, and is associated with decreased antigen presentation, cytokine production and changes in phagocytosis, and mediated by epigenetic and metabolic factors (Pfortmueller et al., 2017)(Saeed et al., 2014)(Cheng et al., 2014). These immune disruptions associated with low

HLA-DR may contribute to impaired clearance of pathological proteins, neuronal dysfunction and subsequent cognitive and motor impairment. In contrast, PD animal models involving acute toxin/protein injections/pathology suggest deleterious effects of increased HLA-DR (Williams et al., 2018)(Harms et al., 2013). This may indicate that in the acute situation seen in animal models, the detrimental effects of HLADR (e.g.pro-inflammatory cytokine release) outweigh the beneficial effects of increased antigen presentation/clearance, whereas in the chronic clinical situation, the beneficial effects of increased HLA-DR mediated pathology clearance outweigh the detrimental effects. However, more detailed prospective studies will be required to further investigate these effects and hypotheses.

The PD-control marker changes seen in total monocytes may mainly reflect changes seen in the pre-dominant classical monocyte subtype. However, analysis of the more limited data from Intermediate and Non-Classical monocytes also indicated broadly similar trends in these subtypes overall (Appendix A). Further detailed studies specifically investigating monocyte subtype and related innate immune cell (e.g. dendritic cell) changes in PD will be important in future work.

4.2 Serum Endotoxin

To our knowledge, this is the first study to directly demonstrate elevated serum endotoxin in PD, particularly in patients with increased risk for early dementia. Endotoxin is a principal component of the outer membrane of gram-negative bacteria and its major source in serum is translocation of gram-negative bacterial components across gastrointestinal/other mucosal membranes (Bischoff et al., 2014) (Kelesidis et al., 2012)(Alexopoulou et al., 2017) and thus the findings indicate greater bacterial translocation in PD, particularly in the HR group.

Accordingly, previous studies have demonstrated greater gastrointestinal permeability in PD patients, with lower levels of LPS binding protein (LBP) (indicating less LPS neutralisation) and increased gut staining for Escherichia Coli bacteria (Forsyth et al., 2011)(Perez-Pardo et al., 2019). One smaller study (Hasegawa et al., 2015) found no difference in serum endotoxin, but lower LBP (Pal et al., 2015)(Vreugdenhil et al., 2003) in PD patients, suggesting an LPS-LBP imbalance with increased LPS activity. Intestinal microbiome differences are also seen in PD (Scheperjans et al., 2015) and may modulate disease pathology and manifestation (Sampson et al., 2016)(Dodiya et al., 2018).

Low level chronic elevation of serum endotoxin in PD may be an important mediator of innate immune changes. At a cellular level, endotoxin/LPS acts via TLR4, activating NF-κB and transcription of pro-inflammatory cytokines and proteins including pro-IL-1β and NLRP3 (Lu et al., 2008). Intracellular LPS can also activate the non-canonical NLRP3 inflammasome pathway via caspase-11 (caspase-4 or -5 in humans), leading to caspase-1 activation (Man and Kanneganti, 2015)(Stowe et al., 2015). Thus, endotoxin would stimulate both TLR and inflammasome pathways, potentially resulting in cumulative pathogenic effects.

Endotoxin also has direct effects on alpha-synuclein, stimulating increased production in macrophages (Tanji et al., 2002) and specific fibril formation (Kim et al., 2016b)(Bhattacharyya et al., 2019). Furthermore, in-vivo studies have demonstrated synergistic deleterious effects of LPS and alpha-synuclein on PD related pathology and neuronal survival (H.-M. Gao et al., 2011)(Zhang et al., 2018). Amyloid beta and tau pathology, which are additionally related to cognitive impairment, have also been linked to endotoxin-associated inflammation (Asti and Gioglio, 2014)(Kitazawa et al., 2005), with LPS stimulation leading to increased tau production (Bhaskar et al., 2010)(Gardner et al., 2016).

Peripheral endotoxin may also lead to neuroinflammation in the brain, as measured using PET imaging of microglial activation in human subjects following peripheral intravenous injection of low dose LPS (Sandiego et al., 2015). It is unclear whether the microglial activation is a direct consequence of endotoxin in CNS tissues, or of secondary immune cell/protein CNS entry. However, post-mortem studies have found LPS/microbial proteins in relation to amyloid-beta plaques in Alzheimer's disease brains, indicating the presence of endotoxin itself within the brain (Zhan et al., 2016).

As discussed above, variable extent and duration of serum endotoxin exposure (Morris et al., 2015) may also subsequently influence disease pathology through monocyte tolerance and effects on HLA-DR/protein clearance functions (Mukherjee et al., 2015)(Kobayashi et al., 2016)(de Lima et al., 2014), in addition to driving an innate immune response and promoting aggregation, particularly in the HR group.

PCA Component 2 indicated a possible relationship between endotoxin and monocyte TREM2. As discussed above, TREM2 is involved in bacterial clearance (Chen et al., 2013) and may be raised in response to elevated endotoxin and TLR signalling in PD (Hamerman et al., 2006)(Kober and Brett, 2017). Opposite to this elevation seen in HR PD, monocyte TREM2 is decreased in LR PD relative to controls, consistent with the lack of rise in endotoxin/TLR in LR PD. Furthermore, serum endotoxin was positively correlated with sTREM2, which would be consistent with the sTREM2 rise seen with infection related immune activation (Gisslén et al., 2019).

4.3 Alpha-synuclein and Caspase-1

Serum alpha-synuclein and caspase-1 (major factors in PCA component 1), were significantly lower in PD compared to controls regardless of risk group. The study has also discovered a positive relationship between these proteins in serum, plasma and monocyte lysates. This would be consistent with co-accumulation/aggregation and/or parallel changes in production and breakdown.

Alpha-synuclein is physiologically produced, released and taken up by many cells, including peripheral blood cells (Shin et al., 2000)(Barbour et al., 2008)(Tyson et al., 2016) and decreased levels are seen in PD blood (Gupta et al., 2015)(Li et al., 2007)(Ishii et al., 2015) and cerebrospinal fluid (CSF) (Eusebi et al., 2017). This may suggest alpha-synuclein is being sequestered out of bio-fluids by aggregation and/or intracellular accumulation. Higher patient plasma alpha-synuclein found in some studies (Lin et al., 2017)(Duran et al., 2010), may relate to red cell/platelet leakage during centrifugation (Shi et al., 2010).

The decreased monocyte alpha-synuclein release seen in the HR patient group may be an additional contributor to lower serum alpha-synuclein in this group and could relate to exocytosis dysfunction in PD (Lautenschläger et al., 2017)(Logan et al., 2017). Further, increased aggregated alpha-synuclein species found in PD (Parnetti et al., 2019) may also cause confounding issues with detection by the immunoassays used.

Caspase-1, a key component of the inflammasome pathway (Strowig et al., 2012), is produced by many cell types, including monocytes (Shamaa et al., 2015). Activation of inflammasome complexes (e.g. Nucleotide-binding domain, leucine rich repeat containing receptor family pyrin domain containing-3(NLRP3)) (Strowig et al., 2012)(Man and Kanneganti, 2015), triggered by a variety of stimuli related to homeostatic disruption (e.g. microbial/viral RNA/DNA components, ATP, uric acid) (Man and Kanneganti, 2015), leads to activation of

caspase-1, which subsequently cleaves other proteins (e.g. pro-IL-1β, pro-IL-18), leading to inflammation.

Activated caspase-1 can also cleave alpha-synuclein, making it more aggregable (Wang et al., 2016) and our observation of decreased serum caspase-1 and its correlation with alpha-synuclein may suggest they are both being sequestered out of serum, possibly into cells or aggregates, as a common process in PD. Studies, including our own work (White et al., 2018), have also shown that alpha-synuclein can activate inflammasome pathways causing inflammatory cytokine production (Codolo et al., 2013)(Zhou et al., 2016). Hence both alpha-synuclein and caspase-1 may interact in a bidirectional loop, which contributes to both increased inflammation and intracellular alpha-synuclein aggregation in PD.

In contrast to the current study, Zhou et al. found increased caspase-1 in a smaller cohort of twelve patients compared to controls (Zhou et al., 2016). However, differences in patient/control demographics and longer delays prior to higher speed centrifugation (increasing leakage risk of intracellular caspase-1) in that study, may have contributed to the differences.

The alpha-synuclein and caspase-1 related monocyte assays may additionally suggest functional impairment of monocytes in PD. Previous studies have found TLR4-mediated stimulation of microglial phagocytosis and alpha-synuclein uptake (Fellner et al., 2013)(Venezia et al., 2017) and increased caspase-1 release on endotoxin stimulation of PBMCs (White et al., 2018). However, PD monocytes in this study demonstrated no increased alpha-synuclein uptake or LPS-induced caspase-1 secretion, contrary to what might be expected given their higher TLR4+ percentage, compared to controls.

4.4 Relevance of peripheral immune changes to PD pathology

Peripheral changes in alpha-synuclein and innate immune and microbial related molecules may provide relevant insights into PD pathogenesis and heterogeneity. In particular, multiple routes of communication between the CNS and periphery, (including lymphatic routes (Louveau et al., 2015), blood/brain barrier, choroid plexus, CSF, meninges and the peripheral/autonomic nervous system (Su and Federoff, 2014)), indicate that peripheral changes could be influenced by and/or influence CNS pathology. Importantly, peripheral LPS injection in humans leads to rapid central microglial activation on PET imaging and highlights the strength of influence of peripheral immune factors on the CNS (Sandiego et al., 2015).

Alpha-synuclein pathology is present in the gut and periphery as well as the brain in PD (Forsyth et al., 2011) and some of the peripheral immune changes observed may be directly reflective of such pathology. Also, peripheral factors such as the microbiome (e.g. gut) may have parallel peripheral immune and CNS effects (Marizzoni et al., 2017), including in PD (Scheperjans et al., 2015)(Unger et al., 2016).

In addition to potential direct contributions towards the pathology, peripheral monocytes constitute an easily repeatedly accessible source of cells from a living patient and may provide insights into generic cellular processes disrupted in PD. While monocytes are considered to contribute towards choroid plexus macrophages (Kierdorf et al., 2019), genetic variations in central microglia function have been paralleled in related peripheral monocytes (Bradshaw et al., 2013), indicating that monocytes could act as peripheral proxies or models for particular aspects of study of microglia and CNS innate immune cells in PD.

4.5 Limitations

Our sample size was limited by the feasibility of collecting patient-control samples paired by age, gender and *MAPT* haplotype for parallel processing of samples. Although this was advantageous in terms of ensuring that each patient-control pair experienced minimal variations due to methodological issues, it limited power which may explain our inability to detect previously observed differences in inflammatory cytokines(Williams-Gray et al., 2016)(Qin et al., 2016). In addition, despite practical corrections for multiple comparison testing, we cannot exclude the possibility of Type I errors.

Dopamine may influence immune cell properties (Papa et al., 2017) and Levodopa/dopaminergic medications could therefore cause potential confounding effects. However, none of the measured markers had any relationship with the Levodopa equivalent dose.

4.6 Conclusions

The observed changes in monocyte and serum markers indicate significant innate immune involvement in early-moderate PD, with differential and more marked effects in those with greater clinical impairment and at increased risk for early cognitive decline, suggesting that certain immune changes may be relevant to faster disease progression. Relevant mechanistic pathways and hypothesized interactions are summarised in Fig.6.

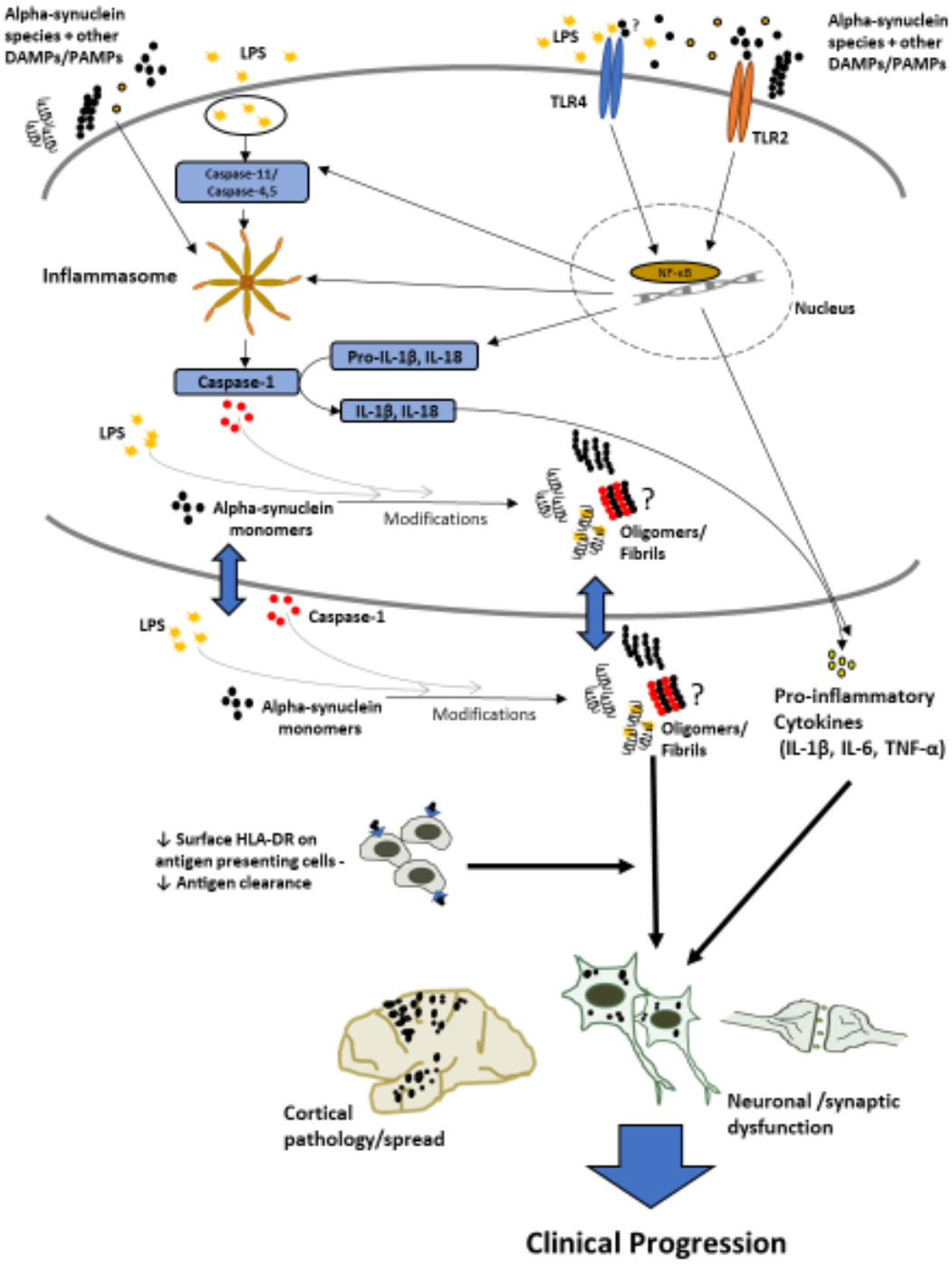

Figure 6 – Summary

Schematic diagram of key innate immune related markers, pathological pathways and hypothesised interactions relevant to clinical progression in Parkinson's disease, based on insights from this study and previous literature. The cellular section represents any cell in which the relevant markers/processes are present. The outcomes of these processes, together

with decreased clearance and circulatory spread, could ultimately contribute towards increased neuronal/synaptic dysfunction, cortical pathology, and consequent cognitive/clinical progression.

LPS – Lipopolysaccharide (Endotoxin); DAMPs/PAMPs – Damage/Pathogen Associated Molecular Patterns; NF-κB – Nuclear Factor Kappa B; TREM2- Triggering Receptor Expressed on Myeloid cells-2; HLA-DR- Human Leukocyte Antigen-DR subtype; TLR- Toll-Like Receptor; IL- Interleukin; TNF – Tumour Necrosis Factor.

Higher endotoxin in those patients with higher dementia risk suggests that greater microbial translocation may be an important factor in driving pathology, whilst the association between low monocyte HLA-DR and poor clinical status suggests that impaired antigen presentation may also contribute to increased pathology and neurodegeneration.
Alpha-synuclein and caspase-1 appear to be closely associated and may have reciprocal effects which contribute to inflammasome activation and intracellular alpha-synuclein aggregation in all PD.

The findings need to be replicated and the extent to which the clinical differences are simply correlated with, or are a consequence of, immune changes will require further prospective longitudinal studies. Measurement of serum LBP and other microbial translocation markers (e.g. bactericidal-permeability increasing protein (BPI) (Alexopoulou et al., 2017)), epigenetic markers associated with monocyte endotoxin tolerance and other inflammasome pathway components (e.g. NLRP3 and Apoptosis-associated Speck-like protein containing a C-terminal caspase-recruitment domain (ASC) specks (Gordon et al., 2018)(Franklin et al., 2018)) would provide further insights into involvement of these pathways in PD.

A clearer mechanistic understanding of how innate immune pathways contribute to disease progression and dementia may open up new therapeutic avenues and enable targeted trials of specific immune/microbial related therapies (e.g. caspase-1 /inflammasome inhibitors (Bassil et al., 2016)(Flores et al., 2018)(Coll et al., 2015), TLR antagonists (Lucas and Maes, 2013)(Peri and Piazza, 2012)(Kouli et al., 2019), and gut bacterial translocation reduction therapies (Fukui, 2017)(Gangarapu et al., 2015)) in particular subgroups. Improving constipation/gastrointestinal health, and prevention/early treatment of infections may also be of relevance, while specific markers may have additional value as biomarkers to monitor target engagement of immune-directed therapies. Further detailed investigation of the components and relationships highlighted in this study will be essential for progression towards such clinical and therapeutic applications.

5. Acknowledgements

We gratefully acknowledge the participation of all our patient and control volunteers and NIHR Cambridge BioResource volunteers and thank the NIHR Cambridge BioResource centre and staff for their contribution. We thank the National Institute for Health Research and NHS Blood and Transplant. We also acknowledge the support of the Cambridge NIHR BRC Cell Phenotyping Hub and the Core Biochemical Assay Laboratory at Cambridge University Hospitals.

6. Funding

Funding for this work was provided by Addenbrooke's Charitable Trust (PF15/CWG), the Rosetrees Trust (M369-F1) and the NIHR Cambridge Biomedical Research Centre (146281). RSW was supported by a Fellowship from Addenbrooke's Charitable Trust (RG77199, PF19/CWG). DKV was supported by a Junior Research Fellowship from Homerton College, Cambridge. KMS was supported by a Fellowship from the Wellcome Trust. WLK is supported by the MRC/UKRI fellowship (MR/S005528/1). DPB is supported by a Wellcome Clinical Research Career Development Fellowship. JJ is supported by the Wellcome Trust (RG79413). RAB is an NIHR Senior Investigator (NF-SI-0616-10011) and is supported by the Wellcome Trust-MRC Cambridge Stem Cell Institute. CHWG is supported by a RCUK/UKRI Research Innovation Fellowship awarded by the Medical Research Council (MR/R007446/1) and by the Cambridge Centre for Parkinson-Plus.

7. Competing Interests

The authors report no competing interests.

8. References

Alexopoulou, A., Agiasotelli, D., Vasilieva, L.E., Dourakis, S.P., 2017. Bacterial translocation markers in liver cirrhosis. Ann. Gastroenterol. 30, 486–497. https://doi.org/10.20524/aog.2017.0178

Asti, A., Gioglio, L., 2014. Can a bacterial endotoxin be a key factor in the kinetics of amyloid fibril formation? J. Alzheimers. Dis. 39, 169–79. https://doi.org/10.3233/JAD-131394

Baba, Y., Kuroiwa, A., Uitti, R.J., Wszolek, Z.K., Yamada, T., 2005. Alterations of T-lymphocyte populations in Parkinson disease. Park. Relat. Disord. 11, 493–498. https://doi.org/10.1016/j.parkreldis.2005.07.005

Barbour, R., Kling, K., Anderson, J.P., Banducci, K., Cole, T., Diep, L., Fox, M., Goldstein, J.M., Soriano, F., Seubert, P., Chilcote, T.J., 2008. Red Blood Cells Are the Major Source of Alpha-Synuclein in Blood. Neurodegener. Dis. 5, 55–59. https://doi.org/10.1159/000112832

Bassil, F., Fernagut, P.-O., Bezard, E., Pruvost, A., Leste-Lasserre, T., Hoang, Q.Q., Ringe, D., Petsko, G.A., Meissner, W.G., 2016. Reducing C-terminal truncation mitigates synucleinopathy and neurodegeneration in a transgenic model of multiple system atrophy. Proc. Natl. Acad. Sci. 113, 9593–9598. https://doi.org/10.1073/pnas.1609291113

Bhaskar, K., Konerth, M., Kokiko-Cochran, O.N., Cardona, A., Ransohoff, R.M., Lamb, B.T., 2010. Regulation of Tau Pathology by the Microglial Fractalkine Receptor. Neuron 68, 19–31. https://doi.org/10.1016/j.neuron.2010.08.023

Bhattacharyya, D., Mohite, G.M., Krishnamoorthy, J., Gayen, N., Mehra, S., Navalkar, A., Kotler, S.A., Ratha, B.N., Ghosh, A., Kumar, R., Garai, K., Mandal, A.K., Maji, S.K., Bhunia, A., 2019. Lipopolysaccharide from Gut Microbiota Modulates α-Synuclein

Aggregation and Alters Its Biological Function. ACS Chem. Neurosci. acschemneuro.8b00733. https://doi.org/10.1021/acschemneuro.8b00733

Bischoff, S.C., Barbara, G., Buurman, W., Ockhuizen, T., Schulzke, J.-D., Serino, M., Tilg, H., Watson, A., Wells, J.M., 2014. Intestinal permeability – a new target for disease prevention and therapy. BMC Gastroenterol. 14, 189. https://doi.org/10.1186/s12876-014-0189-7

Boyette, L.B., Macedo, C., Hadi, K., Elinoff, B.D., Walters, J.T., Ramaswami, B., Chalasani, G., Taboas, J.M., Lakkis, F.G., Metes, D.M., 2017. Phenotype, function, and differentiation potential of human monocyte subsets. PLoS One 12, e0176460. https://doi.org/10.1371/journal.pone.0176460

Bradshaw, E.M., Chibnik, L.B., Keenan, B.T., Ottoboni, L., Raj, T., Tang, A., Rosenkrantz, L.L., Imboywa, S., Lee, M., Von Korff, A., The Alzheimer Disease Neuroimaging, I., Morris, M.C., Evans, D.A., Johnson, K., Sperling, R.A., Schneider, J.A., Bennett, D.A., De Jager, P.L., Alzheimer Disease Neuroimaging, I., 2013. CD33 Alzheimer's disease locus: altered monocyte function and amyloid biology. Nat Neurosci 16, 848–850. https://doi.org/10.1038/nn.3435

Brochard, V., Combadière, B., Prigent, A., Laouar, Y., Perrin, A., Beray-Berthat, V., Bonduelle, O., Alvarez-Fischer, D., Callebert, J., Launay, J.M., Duyckaerts, C., Flavell, R.A., Hirsch, E.C., Hunot, S., 2009. Infiltration of CD4+ lymphocytes into the brain contributes to neurodegeneration in a mouse model of Parkinson disease. J. Clin. Invest. 119, 182–192. https://doi.org/10.1172/JCI36470

Bryant, C.E., Gay, N.J., Heymans, S., Sacre, S., Schaefer, L., Midwood, K.S., 2015. Advances in Toll-like receptor biology: Modes of activation by diverse stimuli. Crit. Rev. Biochem. Mol. Biol. 50, 359–379. https://doi.org/10.3109/10409238.2015.1033511

Cen, L., Yang, C., Huang, S., Zhou, M., Tang, X., Li, K., Guo, W., Wu, Z., Mo, M., Xiao, Y.,

Chen, X., Yang, X., Huang, Q., Chen, C., Qu, S., Xu, P., 2017. Peripheral Lymphocyte Subsets as a Marker of Parkinson's Disease in a Chinese Population. Neurosci. Bull. 33, 493–500. https://doi.org/10.1007/s12264-017-0163-9

Chang, C.-C., Lin, T.-M., Chang, Y.-S., Chen, W.-S., Sheu, J.-J., Chen, Y.-H., Chen, J.-H., 2018. Autoimmune rheumatic diseases and the risk of Parkinson disease: a nationwide population-based cohort study in Taiwan. Ann. Med. 50, 83–90. https://doi.org/10.1080/07853890.2017.1412088

Chen, Q., Zhang, K., Jin, Y., Zhu, T., Cheng, B., Shu, Q., Fang, X., 2013. Triggering Receptor Expressed on Myeloid Cells-2 Protects against Polymicrobial Sepsis by Enhancing Bacterial Clearance. Am. J. Respir. Crit. Care Med. 188, 201–212. https://doi.org/10.1164/rccm.201211-1967OC

Cheng, S.-C., Quintin, J., Cramer, R.A., Shepardson, K.M., Saeed, S., Kumar, V., Giamarellos-Bourboulis, E.J., Martens, J.H.A., Rao, N.A., Aghajanirefah, A., Manjeri, G.R., Li, Y., Ifrim, D.C., Arts, R.J.W., van der Veer, B.M.J.W., Deen, P.M.T., Logie, C., O'Neill, L.A., Willems, P., van de Veerdonk, F.L., van der Meer, J.W.M., Ng, A., Joosten, L.A.B., Wijmenga, C., Stunnenberg, H.G., Xavier, R.J., Netea, M.G., Netea, M.G., 2014. mTOR- and HIF-1 -mediated aerobic glycolysis as metabolic basis for trained immunity. Science (80-.). 345, 1250684–1250684. https://doi.org/10.1126/science.1250684

Codolo, G., Plotegher, N., Pozzobon, T., Brucale, M., Tessari, I., Bubacco, L., de Bernard, M., 2013. Triggering of Inflammasome by Aggregated α–Synuclein, an Inflammatory Response in Synucleinopathies. PLoS One 8, e55375. https://doi.org/10.1371/journal.pone.0055375

Coll, R.C., Robertson, A.A.B., Chae, J.J., Higgins, S.C., Muñoz-Planillo, R., Inserra, M.C., Vetter, I., Dungan, L.S., Monks, B.G., Stutz, A., Croker, D.E., Butler, M.S., Haneklaus,

M., Sutton, C.E., Núñez, G., Latz, E., Kastner, D.L., Mills, K.H.G., Masters, S.L., Schroder, K., Cooper, M.A., O'Neill, L.A.J., 2015. A small-molecule inhibitor of the NLRP3 inflammasome for the treatment of inflammatory diseases. Nat. Med. 21, 248–255. https://doi.org/10.1038/nm.3806

de Lima, T.M., Sampaio, S.C., Petroni, R., Brigatte, P., Velasco, I.T., Soriano, F.G., 2014. Phagocytic activity of LPS tolerant macrophages. Mol. Immunol. 60, 8–13. https://doi.org/10.1016/j.molimm.2014.03.010

Dodiya, H.B., Forsyth, C.B., Voigt, R.M., Engen, P.A., Patel, J., Shaikh, M., Green, S.J., Naqib, A., Roy, A., Kordower, J.H., Pahan, K., Shannon, K.M., Keshavarzian, A., 2018. Chronic stress-induced gut dysfunction exacerbates Parkinson's disease phenotype and pathology in a rotenone-induced mouse model of Parkinson's disease. Neurobiol. Dis. https://doi.org/10.1016/j.nbd.2018.12.012

Drouin-Ouellet, J., St-Amour, I., Saint-Pierre, M., Lamontagne-Proulx, J., Kriz, J., Barker, R.A., Cicchetti, F., 2015. Toll-like receptor expression in the blood and brain of patients and a mouse model of Parkinson's disease. Int. J. Neuropsychopharmacol. 18. https://doi.org/10.1093/ijnp/pyu103

Duran, R., Barrero, F.J., Morales, B., Luna, J.D., Ramirez, M., Vives, F., 2010. Plasma α-synuclein in patients with Parkinson's disease with and without treatment. Mov. Disord. 25, 489–493. https://doi.org/10.1002/mds.22928

Dzamko, N.L., 2017. LRRK2 and the Immune System, in: Advances in Neurobiology. pp. 123–143. https://doi.org/10.1007/978-3-319-49969-7_7

Eusebi, P., Giannandrea, D., Biscetti, L., Abraha, I., Chiasserini, D., Orso, M., Calabresi, P., Parnetti, L., 2017. Diagnostic utility of cerebrospinal fluid α-synuclein in Parkinson's disease: A systematic review and meta-analysis. Mov. Disord. 32, 1389–1400. https://doi.org/10.1002/mds.27110

Fellner, L., Irschick, R., Schanda, K., Reindl, M., Klimaschewski, L., Poewe, W., Wenning, G.K., Stefanova, N., 2013. Toll-like receptor 4 is required for α-synuclein dependent activation of microglia and astroglia. Glia 61, 349–60. https://doi.org/10.1002/glia.22437

Feuerbach, D., Schindler, P., Barske, C., Joller, S., Beng-Louka, E., Worringer, K.A., Kommineni, S., Kaykas, A., Ho, D.J., Ye, C., Welzenbach, K., Elain, G., Klein, L., Brzak, I., Mir, A.K., Farady, C.J., Aichholz, R., Popp, S., George, N., Neumann, U., 2017. ADAM17 is the main sheddase for the generation of human triggering receptor expressed in myeloid cells (hTREM2) ectodomain and cleaves TREM2 after Histidine 157. Neurosci. Lett. 660, 109–114. https://doi.org/10.1016/j.neulet.2017.09.034

Flores, J., Noël, A., Foveau, B., Lynham, J., Lecrux, C., LeBlanc, A.C., 2018. Caspase-1 inhibition alleviates cognitive impairment and neuropathology in an Alzheimer's disease mouse model. Nat. Commun. 9, 3916. https://doi.org/10.1038/s41467-018-06449-x

Forsyth, C.B., Shannon, K.M., Kordower, J.H., Voigt, R.M., Shaikh, M., Jaglin, J.A., Estes, J.D., Dodiya, H.B., Keshavarzian, A., 2011. Increased intestinal permeability correlates with sigmoid mucosa alpha-synuclein staining and endotoxin exposure markers in early Parkinson's disease. PLoS One 6, e28032. https://doi.org/10.1371/journal.pone.0028032

Franklin, B.S., Latz, E., Schmidt, F.I., 2018. The intra- and extracellular functions of ASC specks. Immunol. Rev. 281, 74–87. https://doi.org/10.1111/imr.12611

Fukui, H., 2017. Gut Microbiome-based Therapeutics in Liver Cirrhosis: Basic Consideration for the Next Step. J. Clin. Transl. Hepatol. 5, 249–260. https://doi.org/10.14218/JCTH.2017.00008

Funk, N., Wieghofer, P., Grimm, S., Schaefer, R., Bühring, H.-J., Gasser, T., Biskup, S., 2013. Characterization of peripheral hematopoietic stem cells and monocytes in Parkinson's disease. Mov. Disord. 28, 392–5. https://doi.org/10.1002/mds.25300

Gangarapu, V., Ince, A.T., Baysal, B., Kayar, Y., Klç, U., Gök, Ö., Uysal, Ö., Şenturk, H., 2015. Efficacy of rifaximin on circulating endotoxins and cytokines in patients with nonalcoholic fatty liver disease. Eur. J. Gastroenterol. Hepatol. 27, 840–845. https://doi.org/10.1097/MEG.0000000000000348

Gao, H.-M., Zhang, F., Zhou, H., Kam, W., Wilson, B., Hong, J.-S., 2011. Neuroinflammation and α-synuclein dysfunction potentiate each other, driving chronic progression of neurodegeneration in a mouse model of Parkinson's disease. Environ. Health Perspect. 119, 807–14. https://doi.org/10.1289/ehp.1003013

Gao, X., Chen, H., Schwarzschild, M.A., Ascherio, A., 2011. Use of ibuprofen and risk of Parkinson disease. Neurology 76, 863–869. https://doi.org/10.1212/WNL.0b013e31820f2d79

Gardai, S.J., Mao, W., Schüle, B., Babcock, M., Schoebel, S., Lorenzana, C., Alexander, J., Kim, S., Glick, H., Hilton, K., Fitzgerald, J.K., Buttini, M., Chiou, S.-S.S., McConlogue, L., Anderson, J.P., Schenk, D.B., Bard, F., Langston, J.W., Yednock, T., Johnston, J.A., 2013. Elevated Alpha-Synuclein Impairs Innate Immune Cell Function and Provides a Potential Peripheral Biomarker for Parkinson's Disease. PLoS One 8, e71634. https://doi.org/10.1371/journal.pone.0071634

Gardner, L.E., White, J.D., Eimerbrink, M.J., Boehm, G.W., Chumley, M.J., 2016. Imatinib methanesulfonate reduces hyperphosphorylation of tau following repeated peripheral exposure to lipopolysaccharide. Neuroscience 331, 72–77. https://doi.org/10.1016/j.neuroscience.2016.06.007

Gerhard, A., Pavese, N., Hotton, G., Turkheimer, F., Es, M., Hammers, A., Eggert, K., Oertel, W., Banati, R.B., Brooks, D.J., 2006. In vivo imaging of microglial activation with [11C](R)-PK11195 PET in idiopathic Parkinson's disease. Neurobiol. Dis. 21, 404–412. https://doi.org/10.1016/j.nbd.2005.08.002

Gisslén, M., Heslegrave, A., Veleva, E., Yilmaz, A., Andersson, L.-M., Hagberg, L., Spudich, S., Fuchs, D., Price, R.W., Zetterberg, H., 2019. CSF concentrations of soluble TREM2 as a marker of microglial activation in HIV-1 infection. Neurol. - Neuroimmunol. Neuroinflammation 6, e512. https://doi.org/10.1212/NXI.0000000000000512

Gordon, R., Albornoz, E.A., Christie, D.C., Langley, M.R., Kumar, V., Mantovani, S., Robertson, A.A.B., Butler, M.S., Rowe, D.B., O'Neill, L.A., Kanthasamy, A.G., Schroder, K., Cooper, M.A., Woodruff, T.M., 2018. Inflammasome inhibition prevents α-synuclein pathology and dopaminergic neurodegeneration in mice. Sci. Transl. Med. 10, eaah4066. https://doi.org/10.1126/scitranslmed.aah4066

Greenland, J.C., Williams-Gray, C.H., Barker, R.A., 2019. The clinical heterogeneity of Parkinson's disease and its therapeutic implications. Eur. J. Neurosci. 49, 328–338. https://doi.org/10.1111/ejn.14094

Grozdanov, V., Bliederhaeuser, C., Ruf, W.P., Roth, V., Fundel-Clemens, K., Zondler, L., Brenner, D., Martin-Villalba, A., Hengerer, B., Kassubek, J., Ludolph, A.C., Weishaupt, J.H., Danzer, K.M., 2014. Inflammatory dysregulation of blood monocytes in Parkinson's disease patients. Acta Neuropathol. 128, 651–63. https://doi.org/10.1007/s00401-014-1345-4

Grozdanov, V., Bousset, L., Hoffmeister, M., Bliederhaeuser, C., Meier, C., Madiona, K., Pieri, L., Kiechle, M., McLean, P.J., Kassubek, J., Behrends, C., Ludolph, A.C., Weishaupt, J.H., Melki, R., Danzer, K.M., 2019. Increased Immune Activation by Pathologic α-Synuclein in Parkinson's Disease. Ann. Neurol. ana.25557. https://doi.org/10.1002/ana.25557

Gupta, V., Garg, R.K., Khattri, S., 2015. Serological Analysis of Alpha-synuclein and NF- κ B in Parkinson's Disease Patients. J. Clin. DIAGNOSTIC Res. 9, BC01-4.

https://doi.org/10.7860/JCDR/2015/12545.5978

Gustot, A., Gallea, J.I., Sarroukh, R., Celej, M.S., Ruysschaert, J.-M., Raussens, V., 2015. Amyloid fibrils are the molecular trigger of inflammation in Parkinson's disease. Biochem. J. 471, 323–333. https://doi.org/10.1042/BJ20150617

Hamerman, J.A., Jarjoura, J.R., Humphrey, M.B., Nakamura, M.C., Seaman, W.E., Lanier, L.L., 2006. Cutting edge: inhibition of TLR and FcR responses in macrophages by triggering receptor expressed on myeloid cells (TREM)-2 and DAP12. J. Immunol. 177, 2051–5. https://doi.org/10.4049/jimmunol.177.4.2051

Hamza, T.H., Zabetian, C.P., Tenesa, A., Laederach, A., Montimurro, J., Yearout, D., Kay, D.M., Doheny, K.F., Paschall, J., Pugh, E., Kusel, V.I., Collura, R., Roberts, J., Griffith, A., Samii, A., Scott, W.K., Nutt, J., Factor, S.A., Payami, H., 2010. Common genetic variation in the HLA region is associated with late-onset sporadic Parkinson's disease. Nat. Genet. 42, 781–785. https://doi.org/10.1038/ng.642

Harms, A.S., Cao, S., Rowse, A.L., Thome, A.D., Li, X., Mangieri, L.R., Cron, R.Q., Shacka, J.J., Raman, C., Standaert, D.G., 2013. MHCII is required for α-synuclein-induced activation of microglia, CD4 T cell proliferation, and dopaminergic neurodegeneration. J. Neurosci. 33, 9592–600. https://doi.org/10.1523/JNEUROSCI.5610-12.2013

Harms, A.S., Delic, V., Thome, A.D., Bryant, N., Liu, Z., Chandra, S., Jurkuvenaite, A., West, A.B., 2017. α-Synuclein fibrils recruit peripheral immune cells in the rat brain prior to neurodegeneration. Acta Neuropathol. Commun. 5, 85. https://doi.org/10.1186/s40478-017-0494-9

Hasegawa, S., Goto, S., Tsuji, H., Okuno, T., Asahara, T., Nomoto, K., Shibata, A., Fujisawa, Y., Minato, T., Okamoto, A., Ohno, K., Hirayama, M., 2015. Intestinal Dysbiosis and Lowered Serum Lipopolysaccharide-Binding Protein in Parkinson's Disease. PLoS One 10, e0142164. https://doi.org/10.1371/journal.pone.0142164

Hu, N., Tan, M.-S., Yu, J.-T., Sun, L., Tan, L., Wang, Y.-L., Jiang, T., Tan, L., 2014. Increased expression of TREM2 in peripheral blood of Alzheimer's disease patients. J. Alzheimers. Dis. 38, 497–501. https://doi.org/10.3233/JAD-130854

Ishii, R., Tokuda, T., Tatebe, H., Ohmichi, T., Kasai, T., Nakagawa, M., Mizuno, T., El-Agnaf, O.M.A., 2015. Decrease in Plasma Levels of α-Synuclein Is Evident in Patients with Parkinson's Disease after Elimination of Heterophilic Antibody Interference. PLoS One 10, e0123162. https://doi.org/10.1371/journal.pone.0123162

Ju, U.-H., Liu, F.-C., Lin, C.-S., Huang, W.-Y., Lin, T.-Y., Shen, C.-H., Chou, Y.-C., Lin, C.-L., Lin, K.-T., Kao, C.-H., Chen, C.-H., Yang, T.-Y., 2019. Risk of Parkinson disease in Sjögren syndrome administered ineffective immunosuppressant therapies. Medicine (Baltimore). 98, e14984. https://doi.org/10.1097/MD.0000000000014984

Kehagia, A. a, Barker, R. a, Robbins, T.W., 2010. Neuropsychological and clinical heterogeneity of cognitive impairment and dementia in patients with Parkinson's disease. Lancet Neurol 9, 1200–1213. https://doi.org/10.1016/S1474-4422(10)70212-X

Kelesidis, T., Kendall, M.A., Yang, O.O., Hodis, H.N., Currier, J.S., 2012. Biomarkers of Microbial Translocation and Macrophage Activation: Association With Progression of Subclinical Atherosclerosis in HIV-1 Infection. J. Infect. Dis. 206, 1558–1567. https://doi.org/10.1093/infdis/jis545

Kierdorf, K., Masuda, T., Jordão, M.J.C., Prinz, M., 2019. Macrophages at CNS interfaces: ontogeny and function in health and disease. Nat. Rev. Neurosci. 20, 547–562. https://doi.org/10.1038/s41583-019-0201-x

Kim, C., Ho, D.-H., Suk, J.-E., You, S., Michael, S., Kang, J., Joong Lee, S., Masliah, E., Hwang, D., Lee, H.-J., Lee, S.-J., 2013. Neuron-released oligomeric α-synuclein is an endogenous agonist of TLR2 for paracrine activation of microglia. Nat. Commun. 4, 1562. https://doi.org/10.1038/ncomms2534

Kim, C., Lee, H.-J., Masliah, E., Lee, S.-J., 2016a. Non-cell-autonomous Neurotoxicity of α-synuclein Through Microglial Toll-like Receptor 2. Exp. Neurobiol. 25, 113. https://doi.org/10.5607/en.2016.25.3.113

Kim, C., Lv, G., Lee, J.S., Jung, B.C., Masuda-Suzukake, M., Hong, C.-S., Valera, E., Lee, H.-J., Paik, S.R., Hasegawa, M., Masliah, E., Eliezer, D., Lee, S.-J., 2016b. Exposure to bacterial endotoxin generates a distinct strain of α-synuclein fibril. Sci. Rep. 6, 30891. https://doi.org/10.1038/srep30891

Kitazawa, M., Oddo, S., Yamasaki, T.R., Green, K.N., LaFerla, F.M., 2005. Lipopolysaccharide-Induced Inflammation Exacerbates Tau Pathology by a Cyclin-Dependent Kinase 5-Mediated Pathway in a Transgenic Model of Alzheimer's Disease. J. Neurosci. 25, 8843–8853. https://doi.org/10.1523/JNEUROSCI.2868-05.2005

Kobayashi, Y., Inagawa, H., Kohchi, C., Okazaki, K., Zhang, R., Soma, G.-I., 2016. Effect of Lipopolysaccharide Derived from Pantoea agglomerans on the Phagocytic Activity of Amyloid β by Primary Murine Microglial Cells. Anticancer Res. 36, 3693–8.

Kober, D.L., Brett, T.J., 2017. TREM2-Ligand Interactions in Health and Disease. J. Mol. Biol. 429, 1607–1629. https://doi.org/10.1016/j.jmb.2017.04.004

Kouli, A., Horne, C.B., Williams-Gray, C.H., 2019. Toll-like receptors and their therapeutic potential in Parkinson's disease and α-synucleinopathies. Brain. Behav. Immun. https://doi.org/10.1016/j.bbi.2019.06.042

Lautenschläger, J., Kaminski, C.F., Kaminski Schierle, G.S., 2017. α-Synuclein – Regulator of Exocytosis, Endocytosis, or Both? Trends Cell Biol. 27, 468–479. https://doi.org/10.1016/j.tcb.2017.02.002

Lee, C.Y.D., Daggett, A., Gu, X., Jiang, L.-L., Langfelder, P., Li, X., Wang, N., Zhao, Y., Park, C.S., Cooper, Y., Ferando, I., Mody, I., Coppola, G., Xu, H., Yang, X.W., 2018. Elevated TREM2 Gene Dosage Reprograms Microglia Responsivity and Ameliorates

Pathological Phenotypes in Alzheimer's Disease Models. Neuron 97, 1032–1048.e5. https://doi.org/10.1016/j.neuron.2018.02.002

Lee, H., James, W.S., Cowley, S.A., 2017. LRRK2 in peripheral and central nervous system innate immunity: its link to Parkinson's disease. Biochem. Soc. Trans. 45, 131–139. https://doi.org/10.1042/BST20160262

Lee, J., Tam, H., Adler, L., Ilstad-Minnihan, A., Macaubas, C., Mellins, E.D., 2017. The MHC class II antigen presentation pathway in human monocytes differs by subset and is regulated by cytokines. PLoS One 12, e0183594. https://doi.org/10.1371/journal.pone.0183594

Li, Q.-X., Mok, S.S., Laughton, K.M., McLean, C.A., Cappai, R., Masters, C.L., Culvenor, J.G., Horne, M.K., 2007. Plasma α-synuclein is decreased in subjects with Parkinson's disease. Exp. Neurol. 204, 583–588. https://doi.org/10.1016/j.expneurol.2006.12.006

Lin, C.-H., Yang, S.-Y., Horng, H.-E., Yang, C.-C., Chieh, J.-J., Chen, H.-H., Liu, B.-H., Chiu, M.-J., 2017. Plasma α-synuclein predicts cognitive decline in Parkinson's disease. J. Neurol. Neurosurg. Psychiatry 88, 818–824. https://doi.org/10.1136/jnnp-2016-314857

Logan, T., Bendor, J., Toupin, C., Thorn, K., Edwards, R.H., 2017. α-Synuclein promotes dilation of the exocytotic fusion pore. Nat. Neurosci. 20, 681–689. https://doi.org/10.1038/nn.4529

Louveau, A., Smirnov, I., Keyes, T.J., Eccles, J.D., Rouhani, S.J., Peske, J.D., Derecki, N.C., Castle, D., Mandell, J.W., Lee, K.S., Harris, T.H., Kipnis, J., 2015. Structural and functional features of central nervous system lymphatic vessels. Nature 523, 337–341. https://doi.org/10.1038/nature14432

Lu, Y.-C., Yeh, W.-C., Ohashi, P.S., 2008. LPS/TLR4 signal transduction pathway. Cytokine 42, 145–151. https://doi.org/10.1016/j.cyto.2008.01.006

Lucas, K., Maes, M., 2013. Role of the Toll Like Receptor (TLR) Radical Cycle in Chronic Inflammation: Possible Treatments Targeting the TLR4 Pathway. Mol. Neurobiol. 48, 190–204. https://doi.org/10.1007/s12035-013-8425-7

Man, S.M., Kanneganti, T.-D., 2015. Regulation of inflammasome activation. Immunol. Rev. 265, 6–21. https://doi.org/10.1111/imr.12296

Marizzoni, M., Provasi, S., Cattaneo, A., Frisoni, G.B., 2017. Microbiota and neurodegenerative diseases. Curr. Opin. Neurol. 30, 630–638. https://doi.org/10.1097/WCO.0000000000000496

McGeer, P.L., McGeer, E.G., 2008. Glial reactions in Parkinson's disease. Mov. Disord. https://doi.org/10.1002/mds.21751

Morris, M.C., Gilliam, E.A., Li, L., 2015. Innate Immune Programing by Endotoxin and Its Pathological Consequences. Front. Immunol. 5, 680. https://doi.org/10.3389/fimmu.2014.00680

Mukherjee, R., Kanti Barman, P., Kumar Thatoi, P., Tripathy, R., Kumar Das, B., Ravindran, B., 2015. Non-Classical monocytes display inflammatory features: Validation in Sepsis and Systemic Lupus Erythematous. Sci. Rep. 5, 13886. https://doi.org/10.1038/srep13886

Nalls, M.A., Plagnol, V., Hernandez, D.G., Sharma, M., Sheerin, U.-M., Saad, M., Simón-Sánchez, J., Schulte, C., Lesage, S., Sveinbjörnsdóttir, S., Stefánsson, K., Martinez, M., Hardy, J., Heutink, P., Brice, A., Gasser, T., Singleton, A.B., Wood, N.W., 2011. Imputation of sequence variants for identification of genetic risks for Parkinson's disease: a meta-analysis of genome-wide association studies. Lancet 377, 641–649. https://doi.org/10.1016/S0140-6736(10)62345-8

Nissen, S.K., Shrivastava, K., Schulte, C., Otzen, D.E., Goldeck, D., Berg, D., Møller, H.J., Maetzler, W., Romero-Ramos, M., 2019. Alterations in Blood Monocyte Functions in

Parkinson’s Disease. Mov. Disord. mds.27815. https://doi.org/10.1002/mds.27815

Ong, S.-M., Hadadi, E., Dang, T.-M., Yeap, W.-H., Tan, C.T.-Y., Ng, T.-P., Larbi, A., Wong, S.-C., 2018. The pro-inflammatory phenotype of the human non-classical monocyte subset is attributed to senescence. Cell Death Dis. 9, 266. https://doi.org/10.1038/s41419-018-0327-1

Pakpoor, J., Noyce, A., Goldacre, R., Selkihova, M., Mullin, S., Schrag, A., Lees, A., Goldacre, M., 2017. Viral hepatitis and Parkinson disease. Neurology 88, 1630–1633. https://doi.org/10.1212/WNL.0000000000003848

Pal, G.D., Shaikh, M., Forsyth, C.B., Ouyang, B., Keshavarzian, A., Shannon, K.M., 2015. Abnormal lipopolysaccharide binding protein as marker of gastrointestinal inflammation in Parkinson disease. Front. Neurosci. 9, 306. https://doi.org/10.3389/fnins.2015.00306

Papa, I., Saliba, D., Ponzoni, M., Bustamante, S., Canete, P.F., Gonzalez-Figueroa, P., McNamara, H.A., Valvo, S., Grimbaldeston, M., Sweet, R.A., Vohra, H., Cockburn, I.A., Meyer-Hermann, M., Dustin, M.L., Doglioni, C., Vinuesa, C.G., 2017. TFH-derived dopamine accelerates productive synapses in germinal centres. Nature 547, 318–323. https://doi.org/10.1038/nature23013

Parmelee, P.A., Thuras, P.D., Katz, I.R., Lawton, M.P., 1995. Validation of the Cumulative Illness Rating Scale in a geriatric residential population. J. Am. Geriatr. Soc. 43, 130–7. https://doi.org/10.1111/j.1532-5415.1995.tb06377.x

Parnetti, L., Gaetani, L., Eusebi, P., Paciotti, S., Hansson, O., El-Agnaf, O., Mollenhauer, B., Blennow, K., Calabresi, P., 2019. CSF and blood biomarkers for Parkinson’s disease. Lancet Neurol. 18, 573–586. https://doi.org/10.1016/S1474-4422(19)30024-9

Patel, A.A., Zhang, Y., Fullerton, J.N., Boelen, L., Rongvaux, A., Maini, A.A., Bigley, V., Flavell, R.A., Gilroy, D.W., Asquith, B., Macallan, D., Yona, S., 2017. The fate and lifespan of human monocyte subsets in steady state and systemic inflammation. J. Exp.

Med. 214, 1913–1923. https://doi.org/10.1084/jem.20170355

Perez-Pardo, P., Dodiya, H.B., Engen, P.A., Forsyth, C.B., Huschens, A.M., Shaikh, M., Voigt, R.M., Naqib, A., Green, S.J., Kordower, J.H., Shannon, K.M., Garssen, J., Kraneveld, A.D., Keshavarzian, A., 2019. Role of TLR4 in the gut-brain axis in Parkinson's disease: a translational study from men to mice. Gut 68, 829–843. https://doi.org/10.1136/gutjnl-2018-316844

Peri, F., Piazza, M., 2012. Therapeutic targeting of innate immunity with Toll-like receptor 4 (TLR4) antagonists. Biotechnol. Adv. 30, 251–260. https://doi.org/10.1016/j.biotechadv.2011.05.014

Pfortmueller, C.A., Meisel, C., Fux, M., Schefold, J.C., 2017. Assessment of immune organ dysfunction in critical illness: utility of innate immune response markers. Intensive Care Med. Exp. 5, 49. https://doi.org/10.1186/s40635-017-0163-0

Qin, X.-Y., Zhang, S.-P., Cao, C., Loh, Y.P., Cheng, Y., 2016. Aberrations in Peripheral Inflammatory Cytokine Levels in Parkinson Disease. JAMA Neurol. 73, 1316. https://doi.org/10.1001/jamaneurol.2016.2742

Racette, B.A., Gross, A., Vouri, S.M., Camacho-Soto, A., Willis, A.W., Searles Nielsen, S., 2018. Immunosuppressants and risk of Parkinson disease. Ann. Clin. Transl. Neurol. 5, 870–875. https://doi.org/10.1002/acn3.580

Rajput, A.H., Voll, A., Rajput, M.L., Robinson, C.A., Rajput, A., 2009. Course in parkinson disease subtypes: A 39-year clinicopathologic study. Neurology 73, 206–212. https://doi.org/10.1212/WNL.0b013e3181ae7af1

Rapsinski, G.J., Wynosky-Dolfi, M.A., Oppong, G.O., Tursi, S.A., Wilson, R.P., Brodsky, I.E., Tükel, Ç., 2015. Toll-Like Receptor 2 and NLRP3 Cooperate To Recognize a Functional Bacterial Amyloid, Curli. Infect. Immun. 83, 693–701. https://doi.org/10.1128/IAI.02370-14

Rayaprolu, S., Mullen, B., Baker, M., Lynch, T., Finger, E., Seeley, W.W., Hatanpaa, K.J., Lomen-Hoerth, C., Kertesz, A., Bigio, E.H., Lippa, C., Josephs, K.A., Knopman, D.S., White, C.L., Caselli, R., Mackenzie, I.R., Miller, B.L., Boczarska-Jedynak, M., Opala, G., Krygowska-Wajs, A., Barcikowska, M., Younkin, S.G., Petersen, R.C., Ertekin-Taner, N.N., Uitti, R.J., Meschia, J.F., Boylan, K.B., Boeve, B.F., Graff-Radford, N.R., Wszolek, Z.K., Dickson, D.W., Rademakers, R., Ross, O.A., 2013. TREM2 in neurodegeneration: evidence for association of the p.R47H variant with frontotemporal dementia and Parkinson's disease. Mol. Neurodegener. 8, 19. https://doi.org/10.1186/1750-1326-8-19

Saeed, S., Quintin, J., Kerstens, H.H.D., Rao, N.A., Aghajanirefah, A., Matarese, F., Cheng, S.-C., Ratter, J., Berentsen, K., van der Ent, M.A., Sharifi, N., Janssen-Megens, E.M., Ter Huurne, M., Mandoli, A., van Schaik, T., Ng, A., Burden, F., Downes, K., Frontini, M., Kumar, V., Giamarellos-Bourboulis, E.J., Ouwehand, W.H., van der Meer, J.W.M., Joosten, L.A.B., Wijmenga, C., Martens, J.H.A., Xavier, R.J., Logie, C., Netea, M.G., Stunnenberg, H.G., 2014. Epigenetic programming of monocyte-to-macrophage differentiation and trained innate immunity. Science (80-.). 345, 1251086–1251086. https://doi.org/10.1126/science.1251086

Sampson, T.R., Debelius, J.W., Thron, T., Janssen, S., Shastri, G.G., Ilhan, Z.E., Challis, C., Schretter, C.E., Rocha, S., Gradinaru, V., Chesselet, M.-F., Keshavarzian, A., Shannon, K.M., Krajmalnik-Brown, R., Wittung-Stafshede, P., Knight, R., Mazmanian, S.K., 2016. Gut Microbiota Regulate Motor Deficits and Neuroinflammation in a Model of Parkinson's Disease. Cell 167, 1469–1480.e12. https://doi.org/10.1016/j.cell.2016.11.018

Sandiego, C.M., Gallezot, J.-D., Pittman, B., Nabulsi, N., Lim, K., Lin, S.-F., Matuskey, D., Lee, J.-Y., O'Connor, K.C., Huang, Y., Carson, R.E., Hannestad, J., Cosgrove, K.P.,

2015. Imaging robust microglial activation after lipopolysaccharide administration in humans with PET. Proc. Natl. Acad. Sci. 112, 12468–12473. https://doi.org/10.1073/pnas.1511003112

Scheperjans, F., Aho, V., Pereira, P.A.B., Koskinen, K., Paulin, L., Pekkonen, E., Haapaniemi, E., Kaakkola, S., Eerola-Rautio, J., Pohja, M., Kinnunen, E., Murros, K., Auvinen, P., 2015. Gut microbiota are related to Parkinson's disease and clinical phenotype. Mov. Disord. 30, 350–358. https://doi.org/10.1002/mds.26069

Schröder, J.B., Pawlowski, M., Meyer zu Hörste, G., Gross, C.C., Wiendl, H., Meuth, S.G., Ruck, T., Warnecke, T., 2018. Immune Cell Activation in the Cerebrospinal Fluid of Patients With Parkinson's Disease. Front. Neurol. 9, 1081. https://doi.org/10.3389/fneur.2018.01081

Scott, K.M., Kouli, A., Yeoh, S.L., Clatworthy, M.R., Williams-Gray, C.H., 2018. A Systematic Review and Meta-Analysis of Alpha Synuclein Auto-Antibodies in Parkinson's Disease. Front. Neurol. 9, 815. https://doi.org/10.3389/fneur.2018.00815

Shamaa, O.R., Mitra, S., Gavrilin, M.A., Wewers, M.D., 2015. Monocyte Caspase-1 Is Released in a Stable, Active High Molecular Weight Complex Distinct from the Unstable Cell Lysate-Activated Caspase-1. PLoS One 10, e0142203. https://doi.org/10.1371/journal.pone.0142203

Shi, M., Zabetian, C.P., Hancock, A.M., Ginghina, C., Hong, Z., Yearout, D., Chung, K.A., Quinn, J.F., Peskind, E.R., Galasko, D., Jankovic, J., Leverenz, J.B., Zhang, J., 2010. Significance and confounders of peripheral DJ-1 and alpha-synuclein in Parkinson's disease. Neurosci. Lett. 480, 78–82. https://doi.org/10.1016/j.neulet.2010.06.009

Shin, E.C., Cho, S.E., Lee, D.K., Hur, M.W., Paik, S.R., Park, J.H., Kim, J., 2000. Expression patterns of alpha-synuclein in human hematopoietic cells and in Drosophila at different developmental stages. Mol. Cells 10, 65–70.

Stevens, C.H., Rowe, D., Morel-Kopp, M.-C., Orr, C., Russell, T., Ranola, M., Ward, C., Halliday, G.M., 2012. Reduced T helper and B lymphocytes in Parkinson's disease. J. Neuroimmunol. 252, 95–99. https://doi.org/10.1016/j.jneuroim.2012.07.015

Stolzenberg, E., Berry, D., Yang, D., Lee, E.Y., Kroemer, A., Kaufman, S., Wong, G.C.L.L., Oppenheim, J.J., Sen, S., Fishbein, T., Bax, A., Harris, B., Barbut, D., Zasloff, M.A., 2017. A Role for Neuronal Alpha-Synuclein in Gastrointestinal Immunity. J. Innate Immun. 9, 456–463. https://doi.org/10.1159/000477990

Stowe, I., Lee, B., Kayagaki, N., 2015. Caspase-11: arming the guards against bacterial infection. Immunol. Rev. 265, 75–84. https://doi.org/10.1111/imr.12292

Strowig, T., Henao-Mejia, J., Elinav, E., Flavell, R., 2012. Inflammasomes in health and disease. Nature 481, 278–286. https://doi.org/10.1038/nature10759

Su, X., Federoff, H.J., 2014. Immune Responses in Parkinson's Disease: Interplay between Central and Peripheral Immune Systems. Biomed Res. Int. 2014, 1–9. https://doi.org/10.1155/2014/275178

Sulzer, D., Alcalay, R.N., Garretti, F., Cote, L., Kanter, E., Agin-Liebes, J., Liong, C., McMurtrey, C., Hildebrand, W.H., Mao, X., Dawson, V.L., Dawson, T.M., Oseroff, C., Pham, J., Sidney, J., Dillon, M.B., Carpenter, C., Weiskopf, D., Phillips, E., Mallal, S., Peters, B., Frazier, A., Lindestam Arlehamn, C.S., Sette, A., 2017. T cells from patients with Parkinson's disease recognize α-synuclein peptides. Nature 546, 656–661. https://doi.org/10.1038/nature22815

Tak, T., van Groenendael, R., Pickkers, P., Koenderman, L., 2017. Monocyte Subsets Are Differentially Lost from the Circulation during Acute Inflammation Induced by Human Experimental Endotoxemia. J. Innate Immun. 9, 464–474. https://doi.org/10.1159/000475665

Tanji, K., Mori, F., Imaizumi, T., Yoshida, H., Matsumiya, T., Tamo, W., Yoshimoto, M.,

Odagiri, H., Sasaki, M., Takahashi, H., Satoh, K., Wakabayashi, K., 2002. Upregulation of alpha-synuclein by lipopolysaccharide and interleukin-1 in human macrophages. Pathol. Int. 52, 572–7. https://doi.org/10.1046/j.1440-1827.2002.01385.x

Tyson, T., Steiner, J.A., Brundin, P., 2016. Sorting out release, uptake and processing of alpha-synuclein during prion-like spread of pathology. J. Neurochem. 139, 275–289. https://doi.org/10.1111/jnc.13449

Unger, M.M., Spiegel, J., Dillmann, K.-U., Grundmann, D., Philippeit, H., Bürmann, J., Faßbender, K., Schwiertz, A., Schäfer, K.-H., 2016. Short chain fatty acids and gut microbiota differ between patients with Parkinson's disease and age-matched controls. Parkinsonism Relat. Disord. 32, 66–72. https://doi.org/10.1016/j.parkreldis.2016.08.019

Venezia, S., Refolo, V., Polissidis, A., Stefanis, L., Wenning, G.K., Stefanova, N., 2017. Toll-like receptor 4 stimulation with monophosphoryl lipid A ameliorates motor deficits and nigral neurodegeneration triggered by extraneuronal α-synucleinopathy. Mol. Neurodegener. 12, 52. https://doi.org/10.1186/s13024-017-0195-7

Vlajinac, H., Dzoljic, E., Maksimovic, J., Marinkovic, J., Sipetic, S., Kostic, V., 2013. Infections as a risk factor for Parkinson's disease: a case–control study. Int. J. Neurosci. 123, 329–332. https://doi.org/10.3109/00207454.2012.760560

Vreugdenhil, A.C.E., Rousseau, C.H., Hartung, T., Greve, J.W.M., van 't Veer, C., Buurman, W.A., 2003. Lipopolysaccharide (LPS)-binding protein mediates LPS detoxification by chylomicrons. J. Immunol. 170, 1399–405. https://doi.org/10.4049/jimmunol.170.3.1399

Wang, W., Nguyen, L.T.T., Burlak, C., Chegini, F., Guo, F., Chataway, T., Ju, S., Fisher, O.S., Miller, D.W., Datta, D., Wu, F., Wu, C.-X., Landeru, A., Wells, J.A., Cookson, M.R., Boxer, M.B., Thomas, C.J., Gai, W.P., Ringe, D., Petsko, G.A., Hoang, Q.Q., 2016. Caspase-1 causes truncation and aggregation of the Parkinson's disease-associated protein α-synuclein. Proc. Natl. Acad. Sci. 113, 9587–9592.

https://doi.org/10.1073/pnas.1610099113

White, A.J., Wijeyekoon, R.S., Scott, K.M., Gunawardana, N.P., Hayat, S., Solim, I.H., McMahon, H.T., Barker, R.A., Williams-Gray, C.H., 2018. The Peripheral Inflammatory Response to Alpha-Synuclein and Endotoxin in Parkinson's Disease. Front. Neurol. 9, 946. https://doi.org/10.3389/fneur.2018.00946

Wijeyekoon, R.S., Kronenberg-Versteeg, D., Scott, K.M., Hayat, S., Jones, J.L., Clatworthy, M.R., Floto, R.A., Barker, R.A., Williams-Gray, C.H., 2018. Monocyte Function in Parkinson's Disease and the Impact of Autologous Serum on Phagocytosis. Front. Neurol. 9, 870. https://doi.org/10.3389/fneur.2018.00870

Williams-Gray, C.H., Evans, J.R., Goris, A., Foltynie, T., Ban, M., Robbins, T.W., Brayne, C., Kolachana, B.S., Weinberger, D.R., Sawcer, S.J., Barker, R.A., 2009. The distinct cognitive syndromes of Parkinson's disease: 5 year follow-up of the CamPaIGN cohort. Brain 132, 2958–2969. https://doi.org/10.1093/brain/awp245

Williams-Gray, C.H., Mason, S.L., Evans, J.R., Foltynie, T., Brayne, C., Robbins, T.W., Barker, R.A., 2013. The CamPaIGN study of Parkinson's disease: 10-year outlook in an incident population-based cohort. J. Neurol. Neurosurg. Psychiatry 84, 1258–64. https://doi.org/10.1136/jnnp-2013-305277

Williams-Gray, C.H., Wijeyekoon, R., Yarnall, A.J., Lawson, R.A., Breen, D.P., Evans, J.R., Cummins, G.A., Duncan, G.W., Khoo, T.K., Burn, D.J., Barker, R.A., ICICLE-PD study group, 2016. Serum immune markers and disease progression in an incident Parkinson's disease cohort (ICICLE-PD). Mov. Disord. 31, 995–1003. https://doi.org/10.1002/mds.26563

Williams-Gray, C.H., Wijeyekoon, R.S., Scott, K.M., Hayat, S., Barker, R.A., Jones, J.L., 2018. Abnormalities of age-related T cell senescence in Parkinson's disease. J. Neuroinflammation 15, 166. https://doi.org/10.1186/s12974-018-1206-5

Williams, G.P., Schonhoff, A.M., Jurkuvenaite, A., Thome, A.D., Standaert, D.G., Harms, A.S., 2018. Targeting of the class II transactivator attenuates inflammation and neurodegeneration in an alpha-synuclein model of Parkinson's disease. J. Neuroinflammation 15, 244. https://doi.org/10.1186/s12974-018-1286-2

Wong, K.L., Yeap, W.H., Tai, J.J.Y., Ong, S.M., Dang, T.M., Wong, S.C., 2012. The three human monocyte subsets: implications for health and disease. Immunol. Res. 53, 41–57. https://doi.org/10.1007/s12026-012-8297-3

Yarnall, A.J., Breen, D.P., Duncan, G.W., Khoo, T.K., Coleman, S.Y., Firbank, M.J., Nombela, C., Winder-Rhodes, S., Evans, J.R., Rowe, J.B., Mollenhauer, B., Kruse, N., Hudson, G., Chinnery, P.F., O'Brien, J.T., Robbins, T.W., Wesnes, K., Brooks, D.J., Barker, R.A., Burn, D.J., ICICLE-PD Study Group, 2014. Characterizing mild cognitive impairment in incident Parkinson disease: The ICICLE-PD Study. Neurology 82, 308–316. https://doi.org/10.1212/WNL.0000000000000066

Zhan, X., Stamova, B., Jin, L.-W., DeCarli, C., Phinney, B., Sharp, F.R., 2016. Gram-negative bacterial molecules associate with Alzheimer disease pathology. Neurology 87, 2324–2332. https://doi.org/10.1212/WNL.0000000000003391

Zhang, W., Gao, J.-H., Yan, Z.-F., Huang, X.-Y., Guo, P., Sun, L., Liu, Z., Hu, Y., Zuo, L.-J., Yu, S.-Y., Cao, C.-J., Wang, X.-M., Hong, J.-S., 2018. Minimally Toxic Dose of Lipopolysaccharide and α-Synuclein Oligomer Elicit Synergistic Dopaminergic Neurodegeneration: Role and Mechanism of Microglial NOX2 Activation. Mol. Neurobiol. 55, 619–632. https://doi.org/10.1007/s12035-016-0308-2

Zhao, J., Han, X., Xue, L., Zhu, K., Liu, H., Xie, A., 2015. Association of TLR4 gene polymorphisms with sporadic Parkinson's disease in a Han Chinese population. Neurol. Sci. 36, 1659–1665. https://doi.org/10.1007/s10072-015-2227-9

Zhao, Y., Wu, X., Li, X., Jiang, L.-L., Gui, X., Liu, Y., Sun, Y., Zhu, B., Piña-Crespo, J.C.,

Zhang, M., Zhang, N., Chen, X., Bu, G., An, Z., Huang, T.Y., Xu, H., 2018. TREM2 Is a Receptor for β-Amyloid that Mediates Microglial Function. Neuron 97, 1023–1031.e7. https://doi.org/10.1016/j.neuron.2018.01.031

Zhou, Y., Lu, M., Du, R.-H., Qiao, C., Jiang, C.-Y., Zhang, K.-Z., Ding, J.-H., Hu, G., 2016. MicroRNA-7 targets Nod-like receptor protein 3 inflammasome to modulate neuroinflammation in the pathogenesis of Parkinson's disease. Mol. Neurodegener. 11, 28. https://doi.org/10.1186/s13024-016-0094-3

Ziegler-Heitbrock, L., Hofer, T.P.J., 2013. Toward a refined definition of monocyte subsets. Front. Immunol. https://doi.org/10.3389/fimmu.2013.00023

9. Figure Legends

Figure 1 – Monocyte subtypes

(A) - Flow cytometry gating strategy for monocytes and monocyte subtypes Singlets are identified by plotting Forward Scatter-Area (FSC-A) versus Forward Scatter-Width (FSC-W) and excluding cells with multiples of a single width size. Monocyte, lymphocytes and granulocytes are distinguished using FSC-A (size) and Side Scatter-Area (SSC-A) (granularity/internal complexity). Monocyte subtypes are distinguished based on CD14 and CD16 expression –Classical (CD14 high, CD16 negative); Intermediate (CD14 high, CD16 positive); Non-Classical (CD14 low, CD16 high).

(B) - Total monocytes (as a percentage of PBMCs) in all patients and controls; overall and within dementia risk groups (Parkinson's disease=red; Controls=yellow).

(C),(D),(E)-Monocyte Subtypes. (C) Classical, (D) Intermediate and (E) Non-Classical monocytes (as percentage of total monocytes) in Parkinson's disease patients and controls; overall and within dementia risk groups (Parkinson's disease=red; Controls=yellow). **significance withstood Bonferroni correction for multiple testing within the relevant category.

Figure 2 – Monocyte surface markers

Total monocyte marker expression in Parkinson's disease cases versus paired controls; overall and within risk groups. Graphs showing total monocyte MFI (Median Fluorescence Intensity) ratios (Test/Isotype) ((A), (C), (E), (G)) and percentage monocytes positive ((B), (D), (F), (H)). (Parkinson's disease=red; Controls=yellow). **significance withstood Bonferroni correction for multiple testing within the relevant category.

Figure 3 – Monocyte HLA-DR expression and clinical data

Relationships between Total Monocyte HLA-DR expression (Test/Isotype MFI Ratio) and clinical data - (A) Semantic Fluency. (B) MDS-UPDRS III motor score. (C) ACE-R score. (D) Absence of correlation with Levodopa equivalent dose.

Figure 4 – Serum markers and Principal Components Analysis

(A)-(E) - Concentrations of serum (A) alpha-synuclein, (B) caspase-1, (C) endotoxin, (D) soluble CD14 and (E) soluble TREM2 in Parkinson's disease patients and controls and within Parkinson's dementia risk groups. (Patients=red; Controls=yellow). **significance withstood Bonferroni correction for multiple testing within the relevant category.

(F)-(H) - Summary of Principal Components Analysis (PCA) component score comparisons between all Parkinson's patients and paired controls and within risk groups. (Patients=red; Controls=yellow).

Component 1 - (+)serum alpha-synuclein, (+)caspase-1 and (-)TLR2+ monocytes; Component 2 - (+)serum endotoxin, (+)monocyte TREM2 and (-)serum alpha-synuclein; Component 3 - (+)classical monocyte percentage and (-)serum alpha-synuclein

Figure 5 – Alpha-synuclein and Caspase-1

(A), (B) - Fluorescence microscope images of monocytes which have taken up fluorescent alpha-synuclein- HiLyteTM Fluor 488 at 90minutes. Hoechst staining identifies cell nuclei. (a) 20X; (b) 40X.

(C), (D) - Monocyte fluorescent alpha-synuclein uptake in standard medium and in autologous serum – (C) percentage alpha-synuclein positive monocytes; (D) total monocyte MFI ratio. (Medium- Patients=35, Controls=35; Serum- Patients=27, Controls=28) (Patients=red; Controls=yellow).

(E),(F),(G),(H) - Alpha-synuclein and caspase-1 in monocyte 24 hour culture supernatants without (E)(F) and with (G)(H) LPS, in all participants and within risk groups. (Patients = red, Controls= yellow).

(All participants- Patients=18, Controls=20; Higher Risk Patients=15, Controls=16; Lower Risk Patients=3, Controls=4) (Patients=red; Controls=yellow).

(I), (J) Graphs showing significant relationship between alpha-synuclein and caspase-1 in serum (I) and monocyte lysates (J).

(K) ICICLE-Cambridge cohort - Relationship between alpha-synuclein and caspase-1 in plasma samples collected at study baseline.

Figure 6 – Summary

Schematic diagram of key innate immune related markers, pathological pathways and hypothesised interactions relevant to clinical progression in Parkinson's disease, based on insights from this study and previous literature. The cellular section represents any cell in which the relevant markers/processes are present. The outcomes of these processes, together with decreased clearance and circulatory spread, could ultimately contribute towards increased neuronal/synaptic dysfunction, cortical pathology, and consequent cognitive/clinical progression.

LPS – Lipopolysaccharide (Endotoxin); DAMPs/PAMPs – Damage/Pathogen Associated Molecular Patterns; NF-κB – Nuclear Factor Kappa B; TREM2- Triggering Receptor Expressed on Myeloid cells-2; HLA-DR- Human Leukocyte Antigen-DR subtype; TLR- Toll-Like Receptor; IL- Interleukin; TNF – Tumour Necrosis Factor.

Peripheral innate immune and bacterial signals relate to clinical heterogeneity in Parkinson's disease

Appendix A

1.Supplementary Methods

1.1 PBMC isolation, Immunocytochemistry and Flow Cytometry

PBMCs were extracted using the standard Ficoll gradient centrifugation method (Ficoll R Paque Plus, GE Healthcare). Cell suspensions obtained following Ficoll gradient separation were centrifuged, and cell pellets were blocked with fluorescence activated cell sorting (FACS) buffer with 2% mouse serum (Sigma) per 0.5–1 × 10^6 cells. Following blocking for 30min, the PBMCs were stained with a panel of conjugated antibodies detailed in Table A.1 and incubated at 4°C for 30min. Following incubation, the PBMCs were washed, fixed with 2% paraformaldehyde (PFA) and then re-suspended in FACS buffer for flow cytometry. Flow cytometry was performed using the BD LSR Fortessa machine with BD FACS Diva software.

Monocytes were gated as described in the literature (Ziegler-Heitbrock and Hofer, 2013) (Givan A.L., Flow cytometry: first principles, 2001) and a minimum number of 10,000 monocyte events were collected per sample. PBMCs from healthy controls, labeled with single conjugated antibodies, were used to determine the appropriate compensation for spectral overlap of fluorophores. Flow cytometry data was analyzed using Flow Jo software, version 10. The percentage of marker positive cells and marker expression levels were determined with reference to isotype control samples (Median Fluorescence Intensity (MFI) Test/Isotype ratio).

The PBMC extractions and staining were performed throughout at 4°C, limiting cell death. During preparatory work for this study, a Live-Dead differentiation stain (LIVE/DEAD™ Fixable Violet Dead Cell Stain, ThermoFisher) was used to assess the percentage of dead cells (Figure A.1). The majority of monocytes (~99.8%) were negative for the Live-Dead stain and positive numbers were not considered to significantly influence the final analysis. Therefore, the Live-Dead stain was not used routinely in this study.

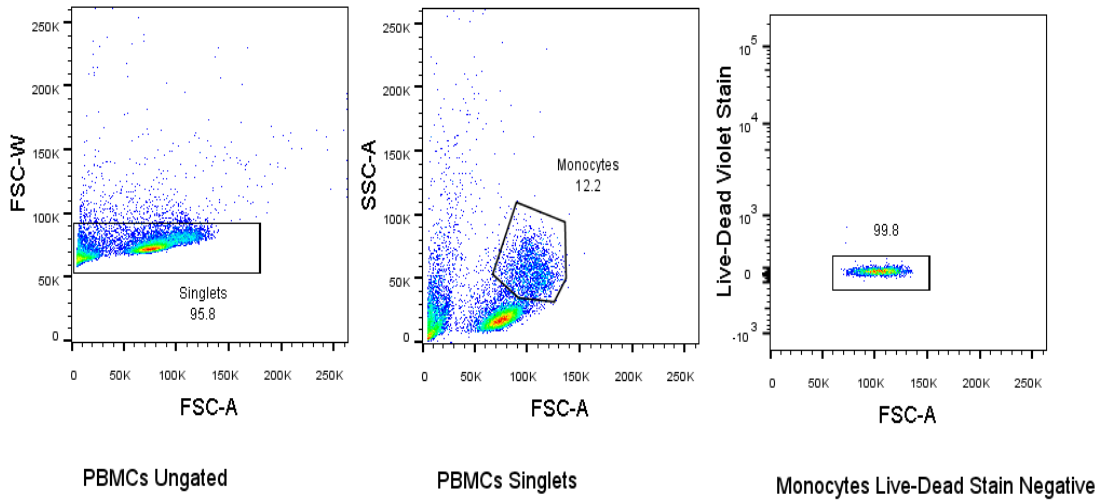

Figure A.1- Live-Dead stain – *Flow cytometry plots demonstrating the use of the Live-Dead stain ex-vivo for estimation of the percentage of dead cells.*

Flow cytometry analysis was performed on total monocytes using a standard method based on a tight gate using the FSC-SSC plot (Figure 1A) (Givan AL. Flow cytometry : first principles. Wiley-Liss 2001)(Tadema et al., 2011), due to the availability of more complete data (problems with the CD14-CD16 staining in a few samples). While this gate may also include a small proportion of related innate immune cells such as dendritic cells, available data indicated that >91% of the FSC-SSC gated monocytes were also monocytes based on CD14-CD16 plot gating.

Additional analysis was performed on Classical (CD14high/CD16negative), Intermediate (CD14high/CD16positive) and Non-Classical (CD14low/CD16high) monocytes. However, the numbers of captured Intermediate and Non-Classical monocytes per sample were considered too low for sufficiently robust analysis and conclusions in this study.

Antibody (anti-Human)	**Isotype Control**	**Volume used (µl)**
CD14 – APC-H7 (MφP9, mouse mAb, BD Biosciences)	Mouse IgG2b κ (27-35, mouse mAb, BD Biosciences)	2
CD16 – PerCP-Cy5.5 (3G8, mouse mAb, BioLegend)	Mouse IgG 1 κ (MOPC-21, mouse mAb, BioLegend)	1
HLA-DR – BV605 (L243, mouse mAb, BioLegend)	Mouse IgG 2a κ (MOPC-173, mouse mAb, BioLegend)	5
TREM2 –APC (#237920, rat mAb, R and D Systems)	Rat IgG 2B (#141945, rat mAb, R and D Systems)	10
TLR2 – PE (TL2.1, mouse mAb, Biolegend)	Mouse IgG 2a κ (MOPC-173, mouse mAb, BioLegend)	5
TLR4 – BV421 (X40, mouse mAb, Biolegend)	Mouse IgG 2a κ (X40, mouse mAb, BD)	5

Table A.1- Antibodies used for immunocytochemistry and flow cytometry.

CD – Cluster of Differentiation; HLA-DR (Human Leukocyte Antigen-DR), TREM2 (Triggering Receptor Expressed on Myeloid cells 2); TLR (Toll like Receptor).

1.2 Serum sample processing and assays

Blood samples taken for serum collection were left to clot for 15 minutes. Samples were centrifuged at 2000rpm for 15 minutes at room temperature. The separated serum was stored in 200-400 µl aliquots and frozen at -80°C.

Mesoscale Discovery (MSD) platform electrochemiluminescence assays (https://www.mesoscale.com).

MSD assay general protocol

Samples were analysed according to the manufacturer's instructions. Briefly, serum samples, stored at -80ºC, were thawed to room temperature. The samples were diluted as specified in the appropriate buffer and loaded in duplicate onto the MSD plates at the specified volume per well. A serial dilution series of manufacturer provided standard samples were also loaded in duplicate. The plate was incubated at room temperature on a shaker for the appropriate time period and washed three times using Phosphate Buffered Saline (PBS) with 0.05% Tween (wash buffer). The specified volume of detection antibody was added at the appropriate concentration and the plate was incubated on the shaker for a further time period. Following removal of the detection antibody, the plate was washed three times and 150µl of 1X or 2X Read buffer was added to each well. Readings were obtained using the MSD SECTOR Imager. Data was exported and analysed using the MSD Discovery Workbench software.

MSD V-Plex Pro-inflammatory panel 1 assay

Samples were analysed for Interferon (IFN)-γ, Interleukin (IL)-1β, IL-2, IL-4, IL-6, IL-8, IL-10, IL-12p70, IL-13 and Tumour Necrosis Factor (TNF)-α in a multiplexed 10-spot 96 well

plate. Samples were diluted 1:2 and used at 50ul per well. 25µl of the detection antibody and 2X Read buffer were used. Both the initial and second incubation times were 2 hours.

MSD V-Plex Human CRP assay

Samples were analysed for C-Reactive protein (CRP) in a single spot 96 well plate. Samples were diluted 1:1000 and used at 25ul per well. 25µl of the detection antibody and 1X Read buffer were used. The initial incubation period was 2 hours, while the second incubation period was 1 hour.

MSD Human Alpha-Synuclein Assay

Samples were analysed for alpha-synuclein in a single spot 96 well plate. Samples were diluted 1:10 and used at 25ul per well. 25µl of the detection antibody was added together with the samples and the plate was incubated only once for 2 hours prior to washing. 2X Read buffer were used.

Serum Endotoxin – Limulus Amoebocyte Lysate (LAL) Assay

The assay was carried out using the Pierce LAL Chromogenic Endotoxin Quantitation Kit (Thermo Scientific) (40 samples) and the LAL Chromogenic Endpoint Assay (Hycult Biotech) (36 samples), due to supplier shortages during the time of performing the assays. Samples from patient and control pairs were analysed in the same plate using the same kit. The results of samples from both batches covered similar ranges (Thermo Scientific kit – 0.46 – 6.32 EU/ml; Hycult Biotech kit – 0.46 – 5.00 EU/ml).

Pierce LAL Chromogenic Endotoxin Quantitation Kit (Thermo Scientific)

The assay was performed in duplicate according to the manufacturer's instructions. Briefly, following pre-incubation of the microplate at 37ºC, 50µL of each standard or sample (diluted 1:50) was inserted into the appropriate microplate well. The plate was covered and incubated for 5 minutes at 37ºC. 50µL of LAL was added to each well following which the plate was incubated at 37ºC for 10 minutes. 100µL of substrate solution was added to each well, followed by incubation at 37ºC for 6 minutes. 50µL of Stop Reagent (25% acetic acid was added and the absorbance at 405-410nm was measured using the FLUOstar Omega microplate reader (BMG LABTECH). The average absorbance of the blank replicates was subtracted from the average absorbance of all individual standard and unknown sample replicates. A standard curve was prepared by plotting the average blank-corrected absorbance for each standard versus its concentration in EU/mL and this was used to determine the endotoxin concentration of each unknown sample.

LAL Chromogenic Endpoint Assay (Hycult Biotech)

The assay was performed in duplicate according to the manufacturer's instructions. Briefly, 50µl of sample (diluted 1:50) or standard was added to the assigned wells. 50µl/well of reconstituted LAL reagent was added and the plate was covered and incubated for 30 minutes at room temperature. The reaction was stopped by adding 50µl 1x stop solution and the absorbance at 405 nm was measured using the FLUOstar Omega microplate reader (BMG LABTECH). A standard curve was prepared by plotting the average blank-corrected absorbance for each standard versus its concentration in EU/mL and this was used to determine the endotoxin concentration of each unknown sample.

Serum Caspase 1 ELISA

Samples were analysed using the Human Caspase 1 Quantikine ELISA kit (R and D Systems). The assay was carried out using the manufacturer's instructions and samples were analysed in duplicate. Samples from patient and control pairs were analysed on the same plate. Briefly, 50µL of Assay Diluent was added to each well, followed by 100µL of Standard or sample applied in duplicate. The plate was incubated for 1.5 hours at room temperature on a shaker, followed by aspiration and three washes with ~400µl of wash buffer per well. 100µL of Caspase-1 Antiserum was added to each well and incubated for 30 minutes at room temperature. The aspiration/wash process was repeated and 100µL of Human Caspase-1 Conjugate was added to each well, followed by a further incubation of 30 minutes. The aspiration/wash process was repeated and 200µL of Substrate Solution was added to each well, followed by 20 minutes incubation protected from light. 50µL of Stop Solution was then added and the optical density of each well was determined within 30 minutes, using the FLUOstar Omega microplate reader (BMG LABTECH) set to 450 nm. Readings at 540 nm or 570 nm were subtracted from the readings at 450 nm to correct for optical imperfections in the plate. In calculating the results, the average zero standard optical density was subtracted from all readings. A standard curve was plotted and used to calculate the caspase-1 concentrations for the samples.

Serum soluble TREM2 ELISA

Samples were analysed using the Cloud-Clone Corp. ELISA kit for TREM2. The assay was carried out using the manufacturer's instructions and samples were analysed in duplicate. Samples from patient and control pairs were analysed on the same plate. Samples were diluted 1:2 with PBS based on the manufacturer's guidance and sample trials.

100µL of standard or sample was added to each well, followed by incubation for 1 hour at 37°C. This was aspirated, followed by the addition of 100µL of Detection Reagent A and further incubation for 1 hour at 37°C. The wells were aspirated and washed three times, followed by the addition of 100µL of Detection Reagent B and a further incubation for 30 minutes at 37°C. The wells were then aspirated and washed five times, followed by the addition of 90µL of Substrate Solution and incubation for 10-20 minutes at 37°C protected from light. 50µL of Stop Solution was then added and the absorbance was read immediately using the FLUOstar Omega microplate reader (BMG LABTECH) at 450nm.

In calculating the results, the average zero standard optical density was subtracted from all readings. A standard curve was plotted and used to calculate the soluble TREM2 concentration in the samples.

Serum soluble CD14 ELISA

Samples were analysed using the Human soluble CD14 Quantikine ELISA kit (R and D systems). The assay was carried out using the manufacturer's instructions and samples were analysed in duplicate. Samples from patient and control pairs were analysed on the same plate. Samples were diluted 1:800 based on the manufacturer's guidance and sample trials. Briefly, 100µL of Assay Diluent was added to each well, followed by 100µL of standard or sample per well in duplicate. The plate was sealed and incubated for 3 hours at room temperature. Following this all wells were aspirated and washed 4 times using ~400µl of Wash Buffer per well. 200µL of Human CD14 Conjugate was added to each well, followed by a further incubation for 1 hour at room temperature. The plate was then washed 4 times as above and 200µL of Substrate Solution was added to each well, followed by incubation for 30 minutes at room temperature, protected from light. 50µL of Stop Solution was added to each well and the

optical density of each well was determined within 30 minutes, using the FLUOstar Omega microplate reader (BMG LABTECH) set to 450 nm.

Readings at 540 nm or 570 nm were subtracted from the readings at 450 nm to correct for optical imperfections in the plate. In calculating the results, the average zero standard optical density was subtracted from all readings. A standard curve was plotted and used to calculate the soluble CD14 concentration in the samples.

1.3 Monocyte separation

CD14+ cells were separated from PBMCs using MACS® magnetic CD14+ beads (Miltenyi Biotec) and "LS" columns, according to the manufacturer's instructions. Both manual and automatic methods of MACS® magnetic bead cell separation (Miltenyi Biotec) were used due to limited availability of equipment. Both methods produced similar results in terms of cell purity and yield. The majority of the samples were separated manually, and all patient and control pairs were separated using the same method.

Manual separation

PBMCs were re-suspended in cooled 'MACS' buffer (1XPBS, 5mg/ml BSA, 2mM EDTA) at a concentration of 80µl/10^7cells. The CD14 magnetic bead suspension (Miltenyi Biotec) was added to the cells at a concentration of 20µl per 10^7 cells and incubated at 4ºC for 30 minutes. The cells were washed and re-suspended in ~1ml of MACS buffer. This was added to a pre-rinsed 'LS' separation column which was placed within the MidiMACS™ magnet separator (Miltenyi Biotec). Once the solution had run through, the column was washed three times with 3ml cool MACS buffer. Finally, the column was removed from the magnet, allowing the magnetic bead labelled cells (CD14+) in the column to be eluted with 5ml of MACS buffer into a 15ml Falcon tube.

Separation using the autoMACS® Pro Separator machine

The autoMACS machine (Miltenyi Biotec) was programmed for CD14 positive selection and the CD14+ beads and the sample and collection tubes were placed appropriately for automatic labelling and separation. The programme was run, and the negative and positive fractions of cells were collected in 15ml Falcon tubes.

1.4 Monocyte uptake assays

Fluorescent alpha-synuclein endocytosis assays

Titration and time course experiments were performed prior to the start of the study to optimise the concentrations and end time points for the assays.

Uptake assay protocol

CD14+ cells were centrifuged at 350g for 5 minutes and re-suspended in clear RPMI (Roswell Park Memorial Institute culture medium) (Life Technologies) + 10% FCS (Foetal Calf Serum) (Sigma) (200µl per 0.5 x 10^6 monocytes). The cells were placed in 96 well plates at a concentration of 0.5 x 10^6 monocytes in 200ul per well and equilibrated in the incubator (37ºC, 5% CO2) (Test plates) or the fridge (4ºC plates) for 45minutes.

Following this, recombinant human alpha-synuclein (1-140) HiLyte™ Fluor 488 (Anaspec) (2µl of 1µg/µl solution to give a concentration of 10 ng/µl or 10,000ng/ml) was added and mixed into the appropriate wells. The Test plates were placed in the incubator (37ºC, 5% CO2) to simulate in vivo conditions, while the 4ºC plates were placed in the fridge, as monocyte phagocytosis and endocytosis should be inhibited at 4ºC and were used as a reference to account for any non-specific adherence of the proteins to the cells.

The concentration of alpha-synuclein was based on titration experiments, which used concentrations of 100, 1000 and 10,000 ng/ml. Minimising the time period of uptake, while enabling adequate quantification using flow cytometry, required the use of a high concentration of 10,000ng/ml of alpha-synuclein over 90 minutes, which may be representative of localised rises in alpha-synuclein potentially occurring around aggregates, or following cellular disruptions such as the death or lysis of neurones.

At the end of the period of alpha-synuclein incubation (90 minutes), all plates were placed on ice and ~70-90ul of ice cold PBS was added to the well, followed by centrifugation at 350g for 5 min, discarding of the supernatant and re-suspension in 180µl of ice cold PBS. The cells were then transferred to a 96 well V bottomed plate on ice. This was centrifuged at 350g for 5 min and the supernatant was discarded. The remaining cells were washed in FACS buffer and re-suspended in 100µl of 2% PFA to fix the cells. Following incubation for 15-20 minutes, the samples were washed twice, re-suspended in FACS buffer and analysed using flow cytometry.

Flow cytometry

Flow cytometry was performed on the endocytosis assay samples using the BD LSR Fortessa machine and all monocyte events were recorded. Data was processed using Flow Jo software, version 10. The total monocyte percentage positive uptake and MFI ratio values for uptake were calculated based on the 4ºC samples and as described in the Assay Optimisation section below.

Uptake assays in serum medium

The uptake assays described above were also performed simultaneously with the participant's autologous serum, instead of RPMI and 10% FCS. Serum was isolated from blood as described in the Methods section. The extracted serum was kept at 4ºC until use on the same day.

Microscopy

A subset of the monocyte post uptake samples was used for microscopy. A proportion of the fixed monocyte sample was incubated with the nuclear staining Hoechst dye (Thermofisher Scientific) (1:1000) for 30 minutes and then washed with PBS. The cells were re-suspended in PBS and smeared onto a glass slide and air dried with protection from light. A glass cover slip was applied onto the slide with FluorSave™ reagent solution. Fluorescent microscopy was performed using the Leica DM6000 B microscope, using the blue channel (A4 filter cube) for Hoechst and the green channel (L5 filter cube) for fluorescent alpha-synuclein-488.

1.5 Monocyte alpha-synuclein secretion assays

Monocyte culture

Separated monocytes were resuspended in RPMI and 10% FCS at a concentration of $1x10^6$ cells per ml. $1x10^6$ cells were added per well into a 24 well culture plate with and without lipopolysaccharide (LPS)(Sigma) (1ng/ml). The cells were cultured for 24 hours at 37ºC and 5% CO_2. At 24 hours, the contents of each well were removed and centrifuged at 350g for 5 minutes. The supernatant was collected, aliquoted into cryovials and stored at -80ºC.

1.6 Monocyte Lysates

Lysis protocol

Available separated monocytes were homogenized in a solution containing Tris-buffered saline (TBS), 1% Triton X100 (Sigma T8787), Complete protease inhibitor (Roche 04693132001), extraction buffer (AbCam ab193970), and enhancer (AbCam ab193971) on ice for 30 minutes. The resulting solution was centrifuged at 15,000rcf at 4ºC for 20 minutes. The supernatant was removed and assayed for protein concentration.

Bicinchoninic acid (BCA) assay

Protein concentration of the lysates was determined according to the manufacturer's instructions (Pierce 23225). Briefly, 50 parts of Reagent A was mixed with 1 part of Reagent B and appropriate volumes of the mixture were mixed with a protein sample. The resulting solution was incubated at 37ºC for 30 minutes and absorption was measured using the Nanodrop reader. The protein concentration was calculated using a standard curve of protein concentration versus absorbance for the BCA assay.

Western Blots

Western blot protocol

Monocyte lysate samples were mixed with 0.1M dithiothreitol (DTT) and 4X lithium dodecyl sulphate (LDS) at the appropriate volumes and boiled at 70ºC for 10 minutes followed by centrifugation at 13,000rpm for 5 minutes to remove air bubbles. The samples were then loaded onto the wells of a NuPAGE 10% BIS-TRIS gel (Thermofisher) in 1X 3-(N-morpholino) propanesulphonic acid (MOPS) running buffer (Thermofisher NP0001), together with the protein ladder. The gel was run at 85V for 2 hours, 10 minutes and then transferred onto the membrane in 1X Transfer buffer (Thermofisher NP0006)+ 20% methanol.

The membrane was blocked with 5% bovine serum albumin (BSA) or 5% milk in TBS+Tween 20 (Sigma P9416) (TBST) for 1 hour at room temperature, on a shaker. The primary antibody (alpha-synuclein Syn42 (610786, Mouse mAb, BD Bioscience) was added in blocking buffer at the appropriate dilution (alpha-synuclein 1 in 2000) and left overnight at 4ºC on a shaker. On the following day, the primary antibody was washed off 3 x 10 minutes in TBST. The horseradish peroxidase (HRP) conjugated secondary antibody (Sigma A9044) was added in blocking buffer (1 in 5000), followed by incubation for 1 hour at room temperature on a shaker and thorough washing in TBST.

The blot was visualised using the SuperSignal^{TM} kit (Thermofisher). The membrane was placed on top of sealer plastic and a mixture of peroxidase and enhancer was added at a 1:1 ratio on to its surface. This was incubated in the dark for 5 minutes, followed by development of the signal using the UVI TECH Alliance machine.

Following the first staining and visualisation, the membrane was stripped by incubation in Stripping buffer (15g/L glycine (Sigma G8898), 1g/L sodium dodecyl sulphate (Sigma 75746) and 1% v/v Tween 20) for two 30-minute periods, followed by washing in TBST. The membrane was then stained with the caspase-1 antibody (D7F10, Rabbit mAb, Cell Signalling Technology 1/1000; secondary Sigma AP307P, 1/5000) following the same procedure. Subsequently the membrane was stripped again and stained for β-actin (sc-47778, Mouse mAB, Santa Cruz) as the loading control.

The intensity of the appropriate visible bands for both alpha-synuclein and caspase-1 were analysed using Image J software and normalised to β-actin.

2. Assay Optimisation

2.1 Monocyte fluorescent alpha-synuclein uptake assay

The fluorescent alpha-synuclein used (alpha-synuclein (1-140) HiLyte^{TM} Fluor 488) was found to contain 0.75 EU/µl of endotoxin contamination (Lonza Bioscience) due to the manufacturing process. Previous studies have shown that this fluorescence tagged alpha-synuclein product has similar aggregation properties to untagged alpha-synuclein (Anderson and Webb, 2011), but it is possible that the presence of endotoxin may influence certain processes such as fibril formation (Kim et al., 2016). However, the same alpha-synuclein product and conditions were used for all patient and control assays in this study.

Preparatory assays were performed using young control monocytes to optimise the concentration of fluorescent alpha-synuclein used and the time course of the experiment (Figures A.2, A.3, A.4). Fluorescent alpha-synuclein concentrations of 100ng/ml, 1000ng/ml and 10,000ng/ml were trialled at time points of 15, 30, 60 and 90 minutes. As the intention was to minimise the time period of the uptake assays, time points beyond 90 minutes were not tested. A concentration of 10,000ng/ml at the 90-minute time point produced sufficiently distinguishable levels of uptake to use in the final assays.

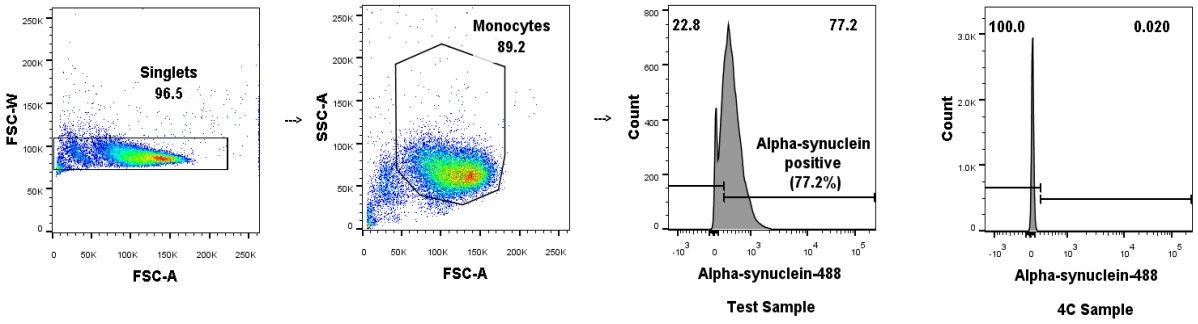

Figure A.2 - Flow cytometry gating strategy for monocyte alpha-synuclein-HiLyte-Fluor-488 uptake. *Monocyte gate extended upwards to include positive monocytes, which may have increased side scatter. Dividing gate on histogram based on position of 4ºC sample. FSC-A=Forward scatter –Area; FSC-W = Forward scatter-width; SSC-A= Side scatter-Area*

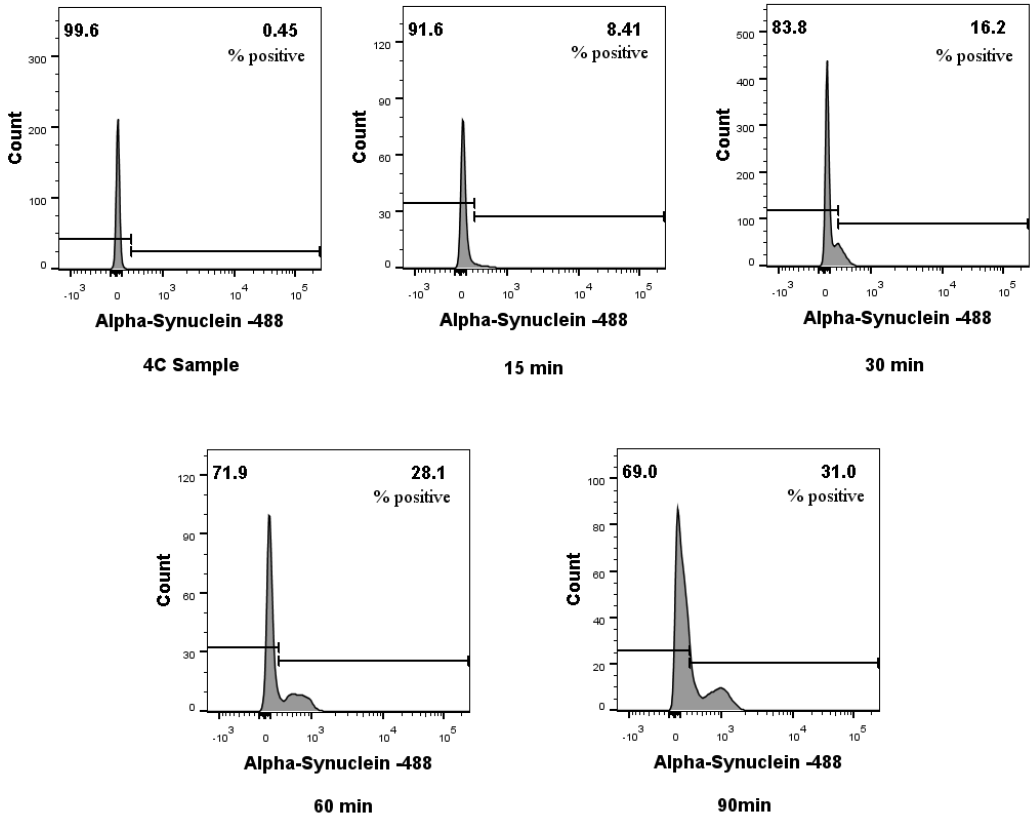

Figure A.3 – Time course of fluorescent alpha-synuclein-488 uptake. *Alpha-synuclein concentration used - 10ng/µl (10,000ng/ml). Subsequent assays were performed at 90 minutes throughout the study. % positive uptake is based on 4ºC sample.*

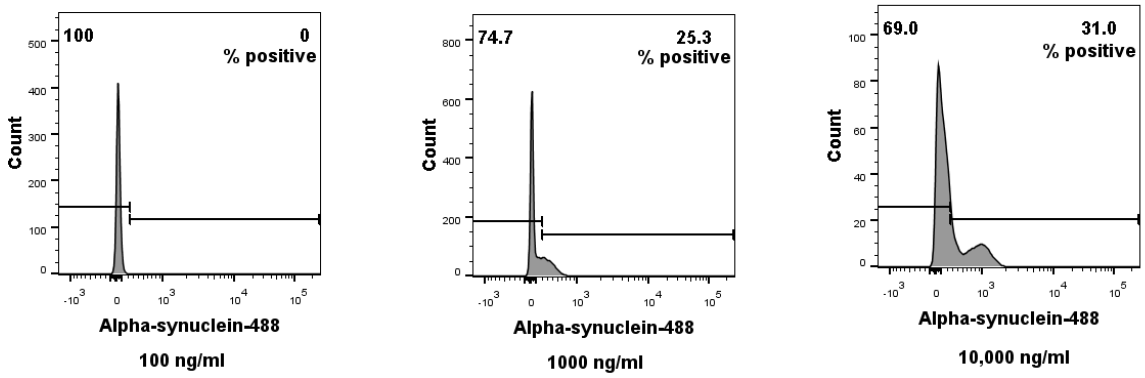

Figure A.4 - Titration of alpha-synuclein concentration. *Examples of uptake at 90-minute time point at concentrations of 100ng/ml, 1000ng/ml and 10,000ng/ml. % positive uptake is based on 4ºC sample.*

The outcomes measured in these fluorescent alpha-synuclein assays included the percentage of monocytes which had taken up alpha-synuclein compared to the 4ºC sample (Test sample % positive - 4ºC sample % positive) and the MFI ratio of total monocytes (Test sample total monocyte MFI/ 4ºC sample MFI).

3. Supplementary Results

3.1 Monocyte subtypes analysis

The Parkinson's disease (PD)-Control differences for each marker in each subtype (Figures A.5, A.6, A.7) showed overall similar trends to that seen in total monocytes (Figure 2). However, the numbers of captured Intermediate (CD14high/CD16positive) and Non-Classical (CD14low/CD16high) monocytes per individual were considered too low for sufficiently robust analysis and conclusions to be made in this study.

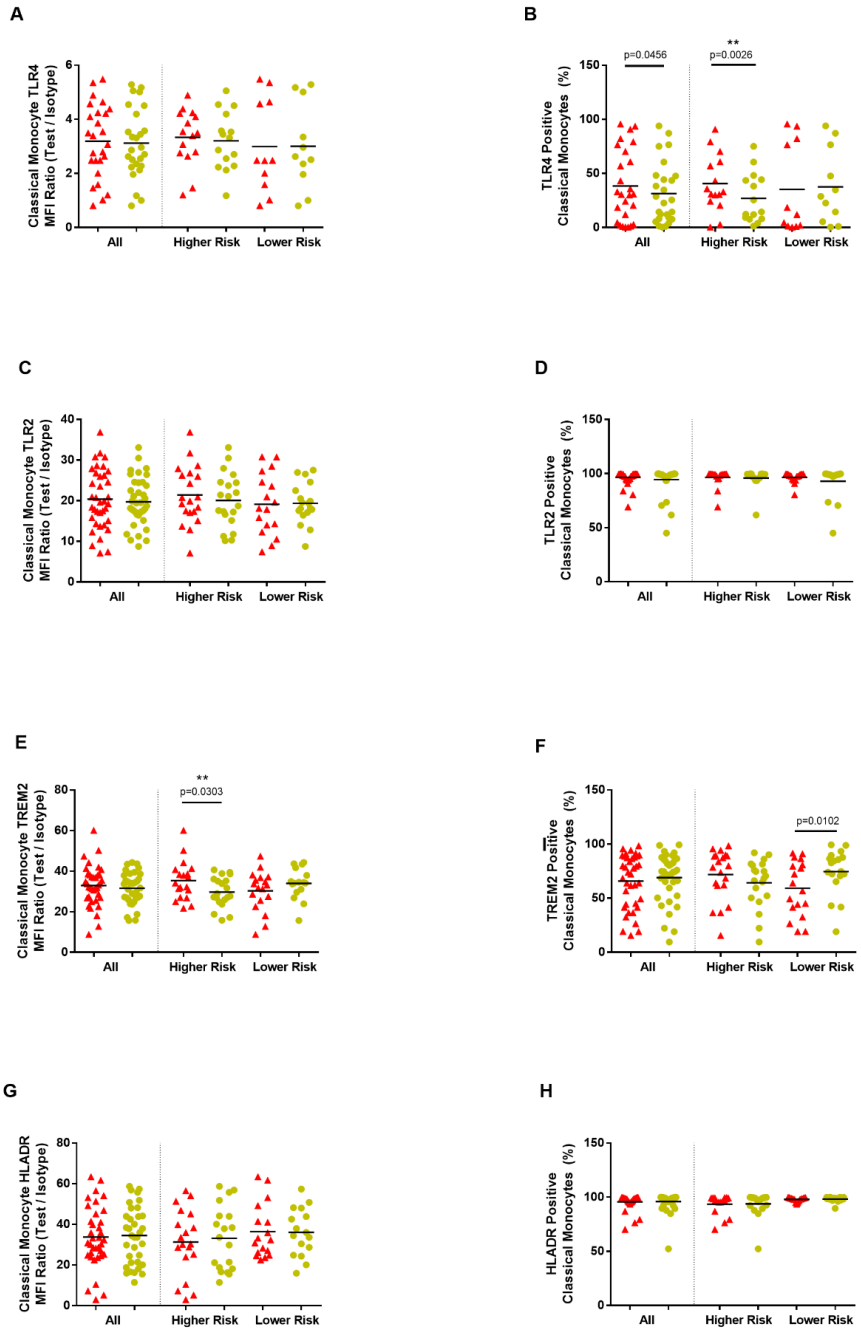

Figure A.5 - Classical monocyte marker expression in Parkinson's disease cases versus paired controls; overall and within risk groups. *Graphs showing Classical monocyte MFI (Median Fluorescence Intensity) ratios (Test/Isotype) ((A), (C), (E), (G)) and percentage Classical monocytes positive ((B), (D), (F), (H)). (Parkinson's disease=red; Controls=yellow). **significance withstood Bonferroni correction for multiple testing within the relevant category.*

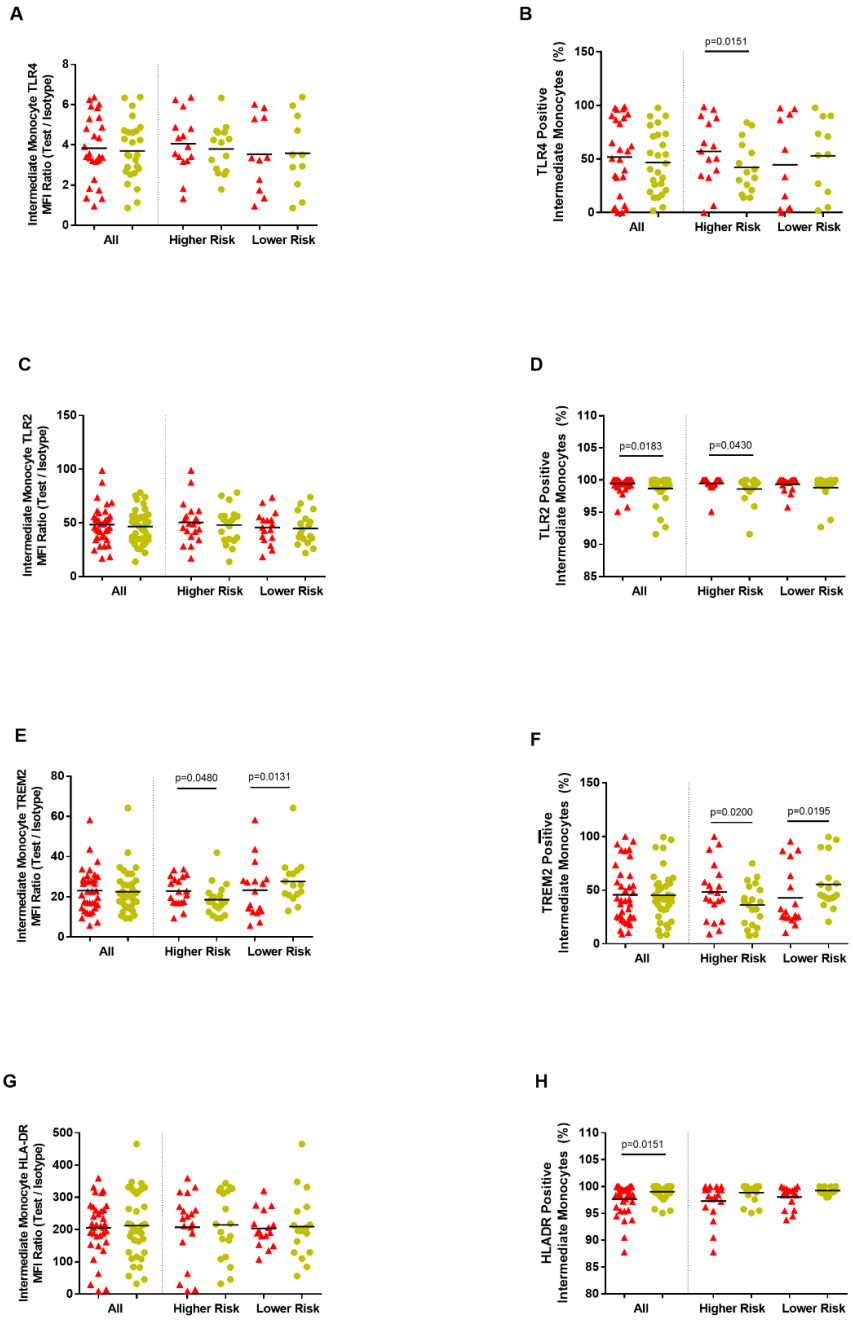

Figure A.6 - Intermediate monocyte marker expression in Parkinson's disease cases versus paired controls; overall and within risk groups. *Graphs showing Intermediate monocyte MFI (Median Fluorescence Intensity) ratios (Test/Isotype) ((A), (C), (E), (G)) and percentage Intermediate monocytes positive ((B), (D), (F), (H)). (Parkinson's disease=red; Controls=yellow). **significance withstood Bonferroni correction for multiple testing within the relevant category.*

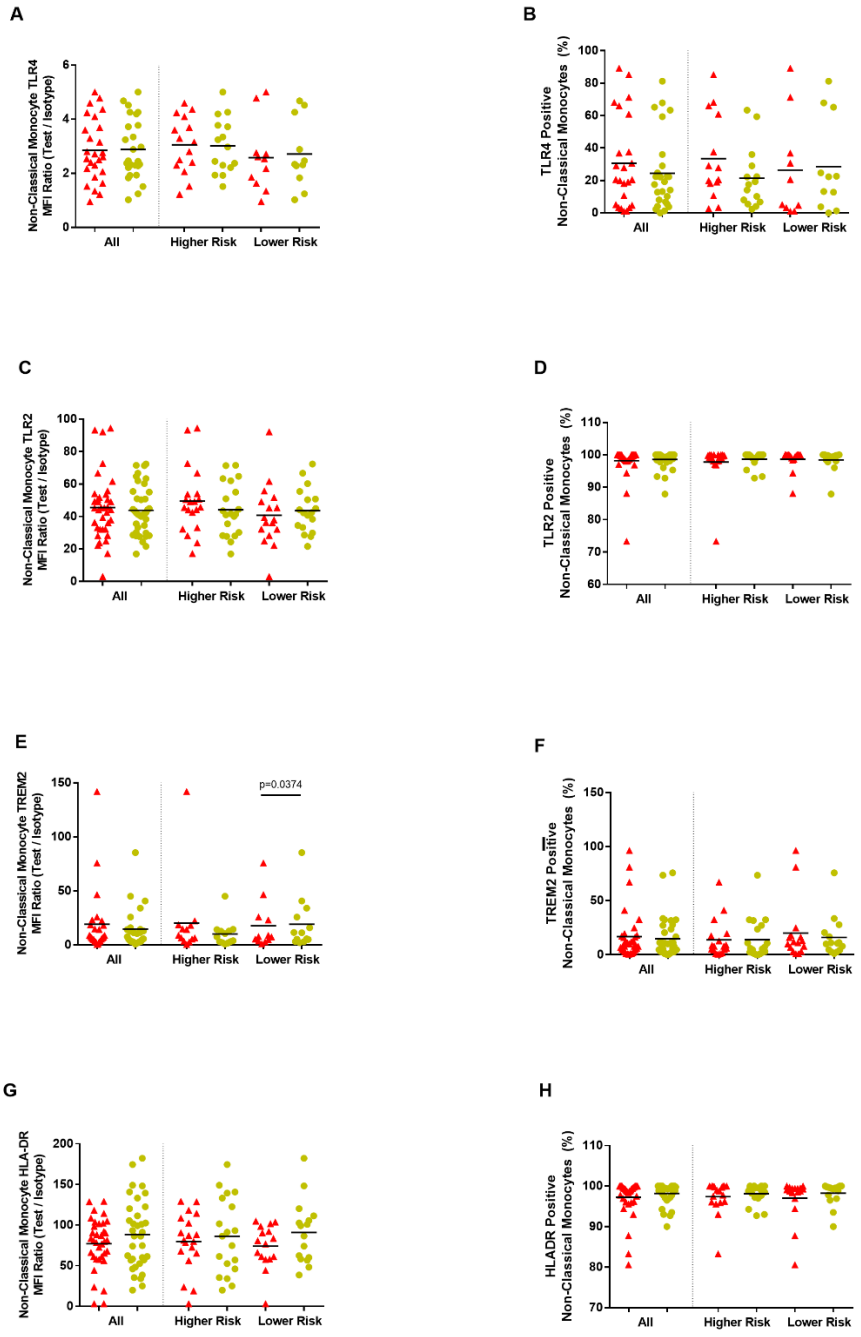

Figure A.7 – Non-Classical monocyte marker expression in Parkinson's disease cases versus paired controls; overall and within risk groups. *Graphs showing Non-Classical monocyte MFI (Median Fluorescence Intensity) ratios (Test/Isotype) ((A), (C), (E), (G)) and percentage Non-Classical monocytes positive ((B), (D), (F), (H)). (Parkinson's disease=red; Controls=yellow). **significance withstood Bonferroni correction for multiple testing within the relevant category.*

3.2 Monocyte markers and associations with clinical and comorbidity variables

Variable (UPDRS motor score)	**Beta Coefficient (B)**	**Significance**	**95% Confidence Interval for B**	
			Lower	**Upper**
Total monocyte HLA-DR	**- 0.308**	**0.022***	**-0.567**	**-0.048**
Age	0.608	0.084	-0.086	1.301
Disease duration	- 1.679	0.359	-5.363	2.005
Levodopa equivalent dose	0.011	0.133	-0.004	0.026
CIRS total score	- 0.902	0.285	-2.594	0.789
(ACE-R score)				
Total monocyte HLA-DR	**0.216**	**0.012***	**0.052**	**0.380**
Age	-0.222	0.314	-0.666	0.221
Disease duration	-0.554	0.640	-2.954	1.846
Levodopa equivalent dose	0.007	0.163	-0.003	0.016
CIRS total score	0.874	0.102	-0.187	1.935
Years of Education	0.431	0.196	-0.236	1.098
(Semantic Fluency)				
Total monocyte HLA-DR	**0.227**	**0.003***	**0.086**	**0.367**
Age	-0.233	0.216	-0.609	0.144
Disease duration	0.894	0.381	-1.162	2.949
Levodopa equivalent dose	0.004	0.328	-0.004	0.012
CIRS total score	0.548	0.219	-0.344	1.440
Years of Education	0.331	0.244	-0.238	0.901

Table A.2 – Monocyte HLA-DR and clinical data - *Results of Linear Regression Analyses with MDS-UPDRS motor score, ACE-R score and Semantic Fluency scores as the dependent variables. CIRS – Cumulative Illness Rating Scale. *p<0.05*

3.3 Serum assay results

Serum MSD Assays

Pro-inflammatory cytokine panel, CRP and alpha-synuclein assays

Serum samples from visit 1, 2 and 3 were used for these assays and equivalent samples from each patient and control pair were analysed within the same experiment. The proteins for which >75% of the samples produced a measurable result across visits (IFN-γ, IL-2, IL-6, IL-8, IL-10, TNF-α, CRP and alpha-synuclein) were included in the analysis.

The average co-efficient of variance for all the assays repeated across the three visits was <1.0. Reliability analysis was performed to calculate the Intraclass correlation coefficient (ICC) estimates and their 95% confidence intervals based on a mean-rating (k=3), absolute-agreement, 2-way mixed-effects model (Koo and Li, 2016). The ICCs for each assay indicated that there was a degree of variability in the results from the three visits (Table A.3). Therefore, the average assay values from the three visits was used for all further analyses of these markers.

Variable	Intraclass Correlation Coefficient (ICC)	95% Confidence Interval	
		Lower	Upper
Serum IFN-γ	0.479	0.201	0.672
Serum IL-2	0.890	0.827	0.933
Serum IL-6	0.442	0.155	0.643
Serum IL-8	0.754	0.635	0.839
Serum IL-10	0.639	0.453	0.769
Serum TNFα	0.777	0.670	0.853
Serum CRP	0.425	0.129	0.632
Serum Alpha-synuclein	0.469	0.196	0.660

Table A.3 -Reliability analysis of serum assays *- Table showing the Intraclass Correlation Coefficients (ICCs) of the serum markers measured at three time points. ICC approaching 1.0 indicates low variability.*

Variable	Group	Parkinson's disease patients	Paired Controls	p
Number (n)	**All**	41	41	
	HR	23	23	
	LR	18	18	
IFN-γ	**All**	6.86 (3.66)	8.63 (4.24)	0.0873
	HR	6.46 (3.32)	9.32 (4.70)	0.0484*
	LR	7.34 (4.07)	7.75 (3.49)	0.7660
IL-2	**All**	0.16 (0.06)	0.17 (0.08)	0.0785
	HR	0.15 (0.06)	0.20 (0.10)	0.0576
	LR	0.15 (0.08)	0.15 (0.07)	0.8653
IL-6	**All**	0.76 (0.42)	0.67 (0.24)	0.1366
	HR	0.86 (0.52)	0.67 (0.25)	0.1069
	LR	0.65 (0.20)	0.66 (0.24)	0.8525
IL-8	**All**	9.84 (2.84)	10.68 (3.24)	0.2604
	HR	9.30 (2.42)	10.24 (1.86)	0.1929
	LR	10.54 (3.23)	11.23 (4.42)	0.6353
IL-10	**All**	0.24 (0.12)	0.26 (0.13)	0.5099
	HR	0.26 (0.13)	0.26 (0.10)	0.8987
	LR	0.22 (0.09)	0.25 (0.16)	0.3692
TNF-α	**All**	2.48 (0.62)	2.66 (0.56)	0.1642
	HR	2.61 (0.67)	2.71 (0.39)	0.5336
	LR	2.31 (0.52)	2.60 (0.73)	0.1928
CRP	**All**	3,797,186.93 (5,798,439.01)	2,672,006.75 (2,091,027.477)	0.6637
	HR	4,591,991.32 (6,751,243.54)	2,953,075.16 (1,974,678.71)	0.7854
	LR	2,825,759.33 (4,360,282.17)	2,328,478,70 (2,233,103.47)	0.6397
Alpha-synuclein	**All**	18,654.48 (6707.89)	33,112.36 (9552.62)	<0.0001**
	HR	18,719.03 (6665.36)	33,629.46 (9084.03)	<0.0001**
	LR	18,567.14 (6969.64)	32,451.61 (10,348.80)	0.0001**

Table A.4 - Summary of serum MSD assay results *(cytokines, CRP and alpha-synuclein). All values indicated are the mean concentration (standard deviation) in pg/ml. Significance (p) indicated is that from paired analysis (parametric paired t-tests - IL-2, IL-6, IL-8, TNF-α; non-parametric Wilcoxon-matched pairs tests – IFN-γ, IL-10, CRP, alpha-synuclein).*

**p<0.05; ** remains significant following correction for multiple testing over all analysed serum markers (12). HR =Higher Risk; LR = Lower Risk.*

3.4 Serum markers and associations with clinical and comorbidity variables

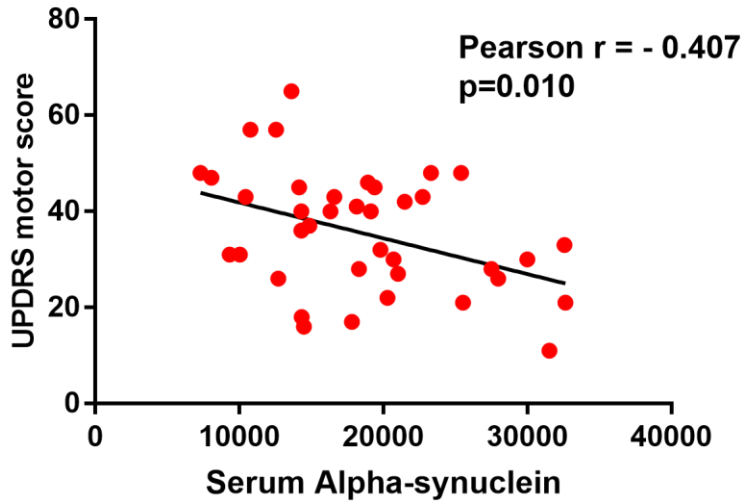

Figure A.8 – Serum alpha-synuclein and motor function *- Scatter plot of serum alpha-synuclein and MDS-UPDRS total motor score.*

Variable	Beta Coefficient (B)	Significance	95% Confidence Interval for B	
			Lower	Upper
Serum alpha-synuclein	-0.001	0.051	-0.001	0.000
Age	0.526	0.124	-0.152	1.204
Disease duration	-1.214	0.502	-4.852	2.424
Levodopa equivalent dose	0.005	0.470	-0.009	0.020
CIRS total score	-0.617	0.467	-2.323	1.089

Table A.5- Serum alpha-synuclein and clinical data. *Linear Regression Analysis with UPDRS motor score as the dependent variable. CIRS – Cumulative Illness Rating Scale.*

3.5 Principal Component Analysis (PCA)

A PCA was run using all participant data on all monocyte markers and the serum markers with uncorrected significant results on overall PD-Control paired analysis. Where more than one measure relating to a factor was significant (e.g. % positive and MFI ratio), the most significant measure for each factor was used for the PCA. Thus, the variables included in the PCA were -: classical monocyte %, monocyte TREM2 MFI ratio, monocyte HLA-DR MFI ratio, TLR2+ monocyte %, TLR4+ monocyte %, serum caspase-1, serum alpha-synuclein, serum endotoxin. The suitability of PCA was assessed prior to analysis. Variables with the lowest Kaiser-Meyer-Olkin (KMO) measures were removed until all the individual KMO measures were greater than 0.55, resulting in the exclusion of TLR4 and HLA-DR from the PCA. The overall KMO

measure for Sampling Adequacy was 0.627. Bartlett's test of sphericity was statistically significant (p=0.001), indicating that the data was likely factorable.

PCA revealed two components that had eigenvalues greater than one and which explained 32.48% and 19.48% of the total variance, respectively. One further component had an eigenvalue > 0.94, explaining a further 15.67% of the variance and visual inspection of the scree plot indicated that three components should be retained. The three-component solution cumulatively explained 67.64% of the total variance. A Varimax rotation with Kaiser normalization was employed to aid interpretability (Table 2).

3.6 Endotoxin and TREM2

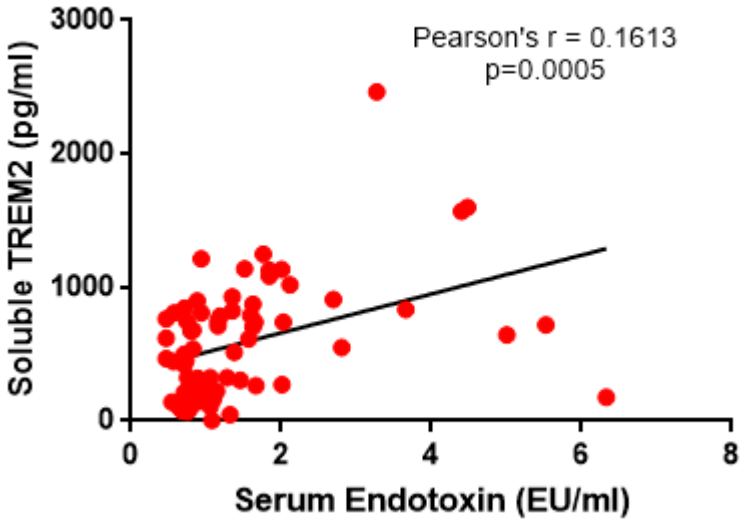

Figure A.9 - Serum endotoxin and soluble TREM2 *- Graph demonstrating a positive relationship between serum endotoxin and soluble TREM2.*

Variable	Beta Coefficient (B)	Significance	95% Confidence Interval for B	
			Lower	Upper
Serum Endotoxin	123.59	0.005	39.80	207.38
Total Monocyte TREM2	-2.52	0.660	-13.96	8.90
Age	15.38	0.083	-2.06	32.84

Table A.6 - Serum endotoxin and soluble TREM2 - *Multiple linear regression analysis with soluble TREM2 as the dependent variable.*

3.7 Alpha-synuclein and Caspase-1

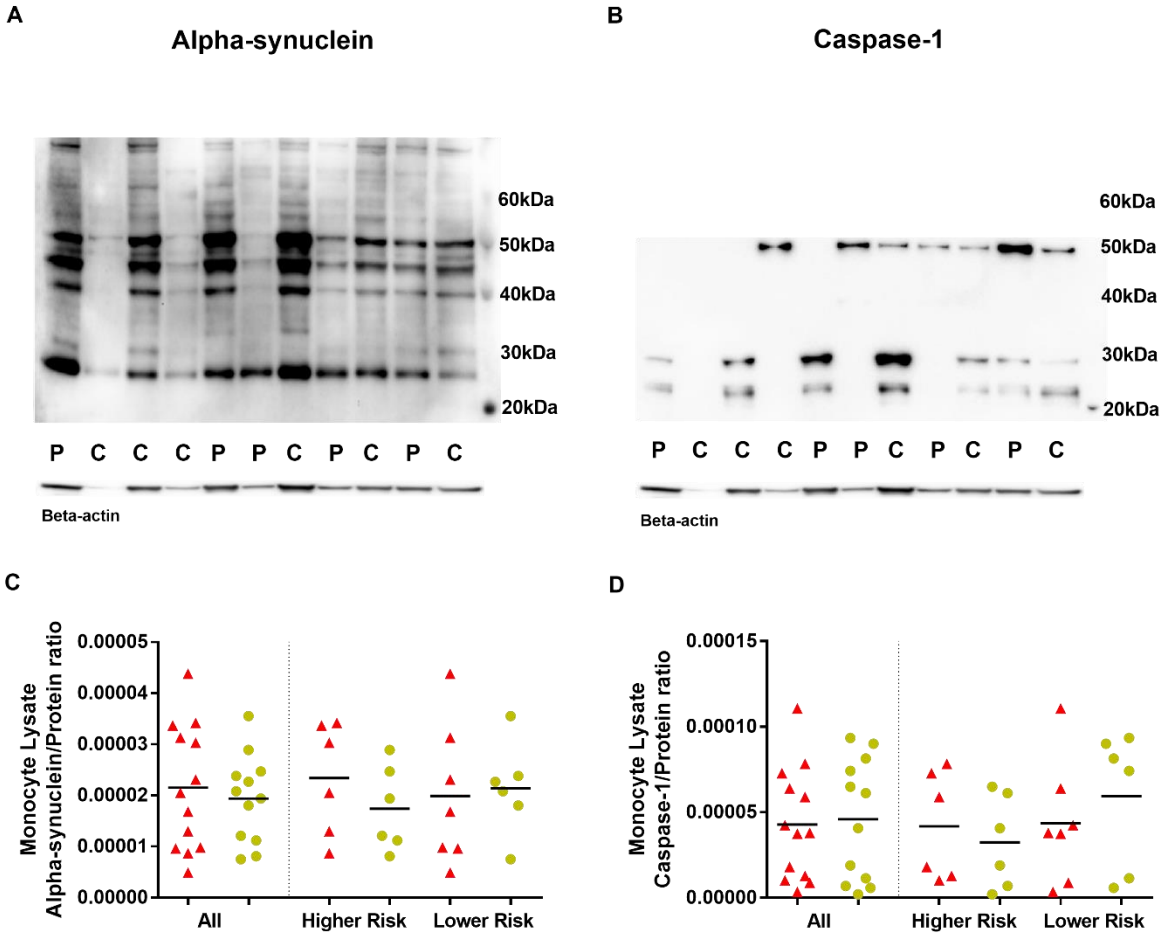

Figure A.10 - Monocyte Lysates *– (A) and (B) Western blots of monocyte lysates for alpha-synuclein (A) and caspase-1 (B), with beta-actin loading control. P=Patient; C=Control. (C) and (D) Monocyte lysate alpha-synuclein (C) and caspase-1 (D) content as a ratio of total protein in patients (red)(n=13) and controls (yellow)(n=12).*

4. Supplementary Data – References

Anderson VL, Webb WW. Transmission electron microscopy characterization of fluorescently labelled amyloid β 1-40 and α-synuclein aggregates. BMC Biotechnol 2011; 11: 125.

Givan AL. Flow cytometry: first principles. Wiley-Liss 2001.

Kim C, Lv G, Lee JS, Jung BC, Masuda-Suzukake M, Hong C-S, et al. Exposure to bacterial endotoxin generates a distinct strain of α-synuclein fibril. Sci Rep 2016; 6: 30891.

Koo TK, Li MY. A Guideline of Selecting and Reporting Intraclass Correlation Coefficients for Reliability Research. J Chiropr Med 2016; 15: 155–163.

Tadema H, Abdulahad WH, Stegeman CA, et al. Increased expression of toll-like receptors by monocytes and natural killer cells in anca-associated vasculitis. PLoS One 2011;6. doi:10.1371/journal.pone.0024315

Ziegler-Heitbrock L, Hofer TPJ. Toward a refined definition of monocyte subsets. Front Immunol 2013; 4